

**ELECTROCHEMICAL STUDIES ON
CHALCOCITE-HEAZLEWOODITE SYSTEM**

M.M. Volkan Bozkurt

**A thesis submitted to the
Faculty of Graduate Studies and Research
in partial fulfillment of the requirements for
the degree of
Master of Engineering**

**Department of Mining and Metallurgical Engineering
McGill University
Montreal, Canada
© January, 1993**

**Anneme, Babama
ve Eşim Ebru'ya Sevgilerimle**

ABSTRACT

Dissolution, rest potential, cyclic voltammetry and contact angle studies have been conducted on the components of INCO matte, chalcocite (Cu_2S) and heazlewoodite (Ni_3S_2), in water and collector solutions.

Dissolution of Ni from heazlewoodite was observed at $\text{pH} < 10$ which decreased to zero at $\text{pH} 12$; Cu dissolution from chalcocite was much less significant. The Ni dissolution mechanism was studied by performing dissolution experiments at $\text{pH} 8$ in air saturated, oxygen saturated and nitrogen-saturated solutions; it was found that dissolution was slightly higher in oxygen-saturated than in air and nitrogen-saturated solutions. It was also found that in the presence of EDTA there was significant additional dissolution of Ni.

Rest potential measurements were conducted over pH range 4 to 12 in the presence and absence of 2×10^{-3} M sodium ethyl xanthate (NaEX) and mercaptobenzothiazole (MBT). Rest potential measurements in water suggested that there could be galvanic interaction between chalcocite (cathode) and heazlewoodite (anode) at low pH values which was suppressed with increasing pH and became zero at $\text{pH} 12$. Rest potential measurements in the presence of NaEX and MBT showed that the effect of collectors on chalcocite was more significant than on heazlewoodite; it was also noted that the rest potential values of the minerals were quite similar in the presence of either NaEX or MBT.

Cyclic voltammetry experiments were carried out on chalcocite and heazlewoodite at $\text{pH} 10$ and 12 ; the minerals showed a significant difference in their response in the presence and absence of collectors. The voltammograms suggested that both NaEX and MBT interact with the

Abstract

minerals in a similar manner, the interaction being more significant in the case of chalcocite than heazlewoodite. A notable reaction was that of NaEX and MBI in suppressing (passivating) the oxidation of chalcocite at potentials > 0.25 V. A reaction for MBT on chalcocite at -0.06 V, not reported previously, was proposed.

Contact angle measurements were performed with chalcocite and heazlewoodite in the presence of 2×10^{-1} M NaEX over a range of potential and pH values. A significant difference in contact angle between chalcocite and heazlewoodite was observed. There was general agreement between cyclic voltammograms and contact angle measurements: For example, the contact angle on Cu_2S in the presence of NaEX increased significantly at the potential range corresponding to passivation. No bubble contact was observed in the presence of 2×10^{-3} M MBT.

RÉSUMÉ

Utilisant des composantes de la matte d'Inco, la chalcocite (Cu_2S) et l'heazlewoodite (Ni_3S_2), on a fait l'étude de dissolution, de potentiel au repos, de voltamétrie cyclique et d'angles de contact en utilisant de l'eau et des solutions contenant des collecteurs.

On note une dissolution de nickel du minéral d'heazlewoodite à $\text{pH} < 10$, dissolution qui décroît pour atteindre zéro à $\text{pH} 12$. La dissolution de la chalcocite est beaucoup moins importante. Le mécanisme de dissolution du nickel fut étudié en exécutant des expériences de dissolution, à $\text{pH} 8$, dans des solutions saturées en air, en oxygène et en azote. On nota un taux de dissolution légèrement plus élevé avec les solutions saturées d'oxygène qu'avec celles saturées en air et en azote. Fait à noter, la présence d'EDTA hausse de façon significative la dissolution de nickel.

Des mesures de potentiel au repos ont été faites avec ou sans la présence d'éthylxanthate de sodium (NaEX) à $2 \times 10^{-4} \text{ M}$ et de mercaptobenzothiazole (MBT) et ce à des pH variant entre 4 et 12. A bas pH et en utilisant de l'eau, les mesures de potentiel au repos suggèrent la possibilité d'une interaction galvanique entre la chalcocite (cathode) et l'heazlewoodite (anode). Cette interaction diminue avec l'accroissement du pH et disparaît complètement à $\text{pH} 12$. En présence de NaEX et de MBT, les mesures de potentiel au repos montrent que l'effet des collecteurs sur la chalcocite est plus important que sur l'heazlewoodite. On a aussi noté que la valeur du potentiel au repos des minéraux était similaire, que ce soit en présence du NaEX ou du MBT.

A des pH de 10 et 12, des expériences de voltamétrie cyclique ont été faites sur la

Résumé

chalcocite et l'heazlewoodite. Avec ou sans collecteurs, les minéraux ont démontré une différence significative dans leur réaction. Les voltammogrammes suggèrent que le NaEX ainsi que le MBT réagissent de façon similaire avec les deux minéraux. L'interaction étant plus importante avec la chalcocite qu'avec l'heazlewoodite. Digne de mention, l'effet suppressif (passivation) du NaEX et du MBT sur l'oxydation de la chalcocite à des potentiels > 0.247 V. Non rapportée précédemment, on propose une réaction du MBT sur la chalcocite à -0.006 V.

En présence de NaEX 2×10^{-4} M et en variant les valeurs de potentiel et de pH, on a fait la mesure d'angles de contact sur la chalcocite et l'heazlewoodite. On a observé une différence significative des angles de contact mesurés sur les deux minéraux. Toutefois, il y a accord entre les voltammogrammes cycliques et les angles de contact mesurés. Par exemple, en présence du NaEX, l'angle de contact du Cu S augmente de façon significative à l'approche du potentiel de passivation. En présence de MBT 2×10^{-4} M, l'angle de contact est de zéro.

ACKNOWLEDGEMENTS

The author would like to thank Professor J. A. Finch and Dr. S. R. Rao for their interest, encouragement and thoughtful advice throughout this project.

The author is grateful to the Incc Ltd for providing funding: He wishes to thank Dr. G. Agar for initiating the project and his advice throughout, and G. Labonté for providing the sample and detail on electrode construction.

The Acknowledgements are further extended to M. Leroux, who supplied the French version of the abstract, all the technical staff of the Mining and Metallurgical Engineering Department, and my colleagues for their friendship and help.

And last but not least, I would like to thank my wife and my parents for their continuous support, encouragement and understanding.

TABLE OF CONTENTS

Abstract	i
Résumé	iii
Acknowledgements	v
Table of Contents	vi
List of Figures	viii
List of Tables	xi

CHAPTER 1. INTRODUCTION

1.1	Basis of Flotation from an Electrochemical View Point	1
1.1.1	Natural floatability	4
1.1.2	Collectorless Flotation	5
1.1.3	Galvanic Interaction	6
1.2	Minerals Studied	9
1.3	Objectives	11

**CHAPTER 2. ELECTROCHEMISTRY IN FLOTATION AND
EXPERIMENTAL SET-UP**

2.1	Fundamental Aspects	14
2.2	Electrochemical Reactions in Sulphide Flotation	16
2.3	Electrodes	19

Table of Contents

2.3.1	Working Electrode	19
2.3.2	Counter Electrode	20
2.3.3	Reference Electrode	20
2.4	Cyclic Voltammetry	21
2.5	Review of Chalcocite-Heazlewoodite System	26
 CHAPTER 3. EXPERIMENTAL PROCEDURE AND RESULTS		
3.1.	Dissolution	28
3.2.	Rest Potential	35
3.3.	Cyclic Voltammetry	40
3.4.	Contact Angle	48
 CHAPTER 4. DISCUSSION		
4.1.	Dissolution	51
4.2.	Rest Potential	52
4.3.	Cyclic Voltammetry	53
4.4.	Contact Angle	59
 CHAPTER 5. CONCLUSION		
5.1.	Dissolution	61
5.2.	Rest Potential	61
5.3.	Cyclic Voltammetry	62
5.4.	Contact Angle	62
	References	64

List of Figures

LIST OF FIGURES

FIGURE 1	Copper Cliff Smelter	12
FIGURE 2	Matte Separation Process	13
FIGURE 3	Massive mineral electrode	19
FIGURE 4	Electrochemical cells	23
FIGURE 5	Schematic representation of potentiostat measurement system	24
FIGURE 6	Cyclic voltammogram of 0.2 M ferrous sulphate at pH 2.5	25
FIGURE 7	Ni dissolution from matte at different pH	31
FIGURE 8	Cu dissolution from matte at different pH	31
FIGURE 9	Ni dissolution from heazlewoodite at different pH	32
FIGURE 10	Cu dissolution from chalcocite at different pH	32
FIGURE 11	Dissolution of chalcocite and heazlewoodite at pH 8	33
FIGURE 12	Dissolution of heazlewoodite at pH 8 in different conditions	33
FIGURE 13	Dissolution of heazlewoodite at pH 8 with and without EDTA	34
FIGURE 14	Rest potentials of chalcocite and heazlewoodite at different pH	37
FIGURE 15	Rest potentials of chalcocite relative to heazlewoodite electrode at different pH	37
FIGURE 16	Rest potentials of chalcocite in the presence and absence of 2×10^{-3} M NaEX at different pH	38
FIGURE 17	Rest potentials of heazlewoodite in the presence and absence of 2×10^{-3} M NaEX at different pH	38
FIGURE 18	Rest potentials of chalcocite in the presence and absence of 2×10^{-3} M MBT at different pH	39

List of Figures

FIGURE 19.	Rest potentials of heazlewoodite in the presence and absence of 2×10^{-3} M MBT at different pH	39
FIGURE 20.	Cyclic voltammograms of heazlewoodite massive electrode in the presence and absence of collectors at pH 10	41
FIGURE 21.	Cyclic voltammograms of heazlewoodite massive electrode in the presence and absence of collectors at pH 12	42
FIGURE 22.	Cyclic voltammogram of single particle chalcocite electrode at pH 9.3 (By Walker et al. (1984))	43
FIGURE 23.	Cyclic voltammograms of chalcocite massive electrode in the presence and absence of 2×10^{-3} M NaEX at pH 9.3	43
FIGURE 24.	Cyclic voltammograms of chalcocite massive electrode in the presence and absence of 2×10^{-3} M NaEX at pH 10	44
FIGURE 25.	Cyclic voltammograms of chalcocite massive electrode in the presence and absence of 2×10^{-3} M NaEX at pH 12	44
FIGURE 26.	Cyclic voltammograms of chalcocite massive electrode in the presence and absence of 2×10^{-3} M MBT at pH 10	45
FIGURE 27.	Cyclic voltammograms of chalcocite massive electrode in the presence and absence of 2×10^{-3} M MBT at pH 12	45
FIGURE 28.	Cyclic voltammograms of heazlewoodite massive electrode in the presence and absence of 2×10^{-3} M NaEX at pH 10	46
FIGURE 29.	Cyclic voltammograms of heazlewoodite massive electrode in the presence and absence of 2×10^{-3} M NaEX at pH 12	46
FIGURE 30.	Cyclic voltammograms of heazlewoodite massive electrode in the presence and absence of 2×10^{-3} M MBT at pH 10	47
FIGURE 31.	Cyclic voltammograms of heazlewoodite massive electrode in the presence and absence of 2×10^{-3} M MBT at pH 12	47
FIGURE 32.	A schematic representation of the captive-bubble contact angle apparatus	48

List of Figures

FIGURE 33. Contact angle values of chalcocite and heazlewoodite as a function of potential in the presence of 2×10^{-3} M NaEX at pH 10	49
FIGURE 34. Contact angle values of chalcocite and heazlewoodite as a function of potential in the presence of 2×10^{-3} M NaEx at pH 12	49
FIGURE 35. Contact angle and current density on chalcocite versus potential	50
FIGURE 36. Contact angle and current density on heazlewoodite versus potential	50

List of Tables

LIST OF TABLES

TABLE 1.	Rest potentials of sulphide minerals at pH 4 and 7	7
TABLE 2.	Dissolution of matte at different pH	28
TABLE 3.	Dissolution of heazlewoodite and chalcocite at different pH	29
TABLE 4.	Dissolution of heazlewoodite at pH 8	29
TABLE 5.	Dissolution of heazlewoodite in the presence and absence of EDTA at pH 8	30
TABLE 6.	Rest potential values of chalcocite and heazlewoodite at different pH	35
TABLE 7.	Rest potential values of chalcocite and heazlewoodite in the presence and absence of collectors at different pH	36
TABLE 8.	Comparison of measured and calculated E_h for chalcocite (anodic peak A_1)	54
TABLE 9.	Comparison of measured and calculated E_h for chalcocite (anodic peak A_2)	56
TABLE 10.	Comparison of measured and calculated E_h for heazlewoodite (anodic peak A_1)	58

CHAPTER 1. INTRODUCTION

1.1. BASIS OF FLOTATION FROM AN ELECTROCHEMICAL VIEW POINT

The fundamental chemical process in flotation is the interaction of a collector with the mineral surface. This process renders the mineral surface hydrophobic and enables the mineral to be held at the air-water interface when gas bubbles are introduced into a pulp and be recovered as the concentrate in the froth phase. Hydrophilic particles remain in the pulp and form the tailing. The froth product is usually the desired mineral, but sometimes it is easier to perform a reverse flotation in which gangue minerals are floated.

The flotation pulp consists of solid mineral particles dispersed in an aqueous solution. An electrical double layer is formed at the solid-solution interface [1]. The collector- mineral interaction takes place in this double layer. In the case of sulphides, the solid phase is a conductor and can gain or lose electrons i.e. can be reduced or oxidized, respectively. In this case electrochemical reactions are expected to play a role, i.e., reactions where electrons are transferred between dissolved species and the mineral across the double layer.

The electrochemical steps of collector (e.g. xanthate) adsorption can be written as follows [2],

First, cathodic reduction of oxygen :



Second, anodic oxidation and adsorption of xanthate, X^- :

CHAPTER 1. INTRODUCTION



More complex mechanisms have been proposed [3, 4], but the reactions above show the basic concept that oxidizing conditions are required for the collector to be adsorbed onto the mineral surface and that dissolved oxygen in the flotation pulp normally provides this condition.

The oxidation-reduction dependence of collector adsorption onto sulphide minerals taken individually is relatively well understood [3]. But, an ore contains more than one sulphide mineral and, in addition wet grinding is often performed with steel grinding media (i.e. rod and ball milling). Hence, it may be expected that interactions among the minerals and the grinding media will occur. These interactions are galvanic and each half-reaction occurs on a different material with the electron transfer occurring during contacts between the two minerals [5].

The presence of a galvanic couple often yields reaction rates which are higher than if each of the minerals were separate. For example, sphalerite (ZnS) is leached by acids at a faster rate when pyrite (FeS₂) is present than when it is alone [6, 7].

The presence of galvanic interactions in flotation may be beneficial or detrimental depending on the minerals present. In some instances, the desired mineral is depressed because of the presence of the couple. Such is the case of galena (PbS) which can be depressed when grinding is performed with a mild steel media [8]. Sometimes, it is the flotation of the non-desired sulphide mineral which is enhanced, for example pyrrhotite in pyrite/pyrrhotite separation [9].

Flotation in the absence of collectors may be induced by electrochemical reactions [10],

CHAPTER 1. INTRODUCTION

11, 12]. It has been shown that if the ore is floatable without collector, its flotation will be selective while the use of a collector will yield less selective flotation, and modifiers are required to regain the original selectivity [13].

When one of the two minerals in the couple is highly soluble it is possible that the ions introduced into the solution will affect the flotation behaviour of the other mineral. One laboratory demonstration of this effect is in the flotation of mixtures of chalcocite (Cu_2S) and pyrite (FeS_2) where the presence of pyrite promoted the dissolution of the chalcocite which released copper ions into solution causing the activation of pyrite [14]. An industrial example is activation of ZnS by Cu solubilized by SO_2 [15].

On the positive side, the adverse effect of the mixture could be inhibited by electrochemical conditioning (application of an electric potential to the minerals) [14]. This is an interesting and potentially important application resulting from an understanding of the electrochemical processes occurring in flotation.

Two means are available for the application of a desired potential to a mineral system. The first one is to use a potentiostat, which is a device capable of applying a controlled potential through the system under study. This is the preferred method for laboratory experimentation [2, 3, 10, 12]. The other method relies on the use of oxidizing or reducing agents to move the electrochemical equilibrium in the desired direction. This is the acting principle behind selective oxidation of one of the minerals in the ore, for example, by potassium permanganate [16].

Following this general description of sulphide flotation, natural floatability, collectorless flotation and galvanic interaction will be discussed in more detail.

CHAPTER 1. INTRODUCTION

1.1.1. Natural floatability:

Natural or inherent floatability of sulphide minerals has always been questioned. Contact angle studies in the '30s showed that sulphide minerals were not inherently hydrophobic since hydrophobicity without collector seemed to be induced by surface contamination [17]

Further studies showed that collectorless flotation occurring after comminution was only possible if the environment was mildly oxidizing [12]. Hence, this could not be related to natural floatability as this property is expected to be independent of the conditions prevailing prior to flotation.

There is one sulphide mineral which is inherently hydrophobic: molybdenite (MoS_2) [18, 19]. The hydrophobic character originates from the crystal structure of the mineral and its preferred cleavage plane. The crystal lattice consists of layers of molybdenum atoms stacked between layers of sulphur atoms. The weakest bond is the S-S bond and the crystal will cleave between two sulphur layers upon impact in comminution. The sulphur atoms, which are hydrophobic, are then exposed on the surface.

Even though other sulphide minerals expose sulphur atoms upon cleavage, the observation of flotation under reducing conditions is possible only if oxygen has been completely excluded from the system [20]. The mineral surfaces expose both sulphur and metal atoms so that only a mild hydrophobic character is imparted to the mineral. This delicate balance appears to be tipped in favour of a hydrophilic character by the formation of hydroxides on the metal cation sites.

CHAPTER 1. INTRODUCTION

1.1.2. Collectorless flotation:

Collectorless flotation should be distinguished from natural flotation. The term "collectorless flotation" is reserved for those cases where a mineral acquires hydrophobicity due to chemical changes at the surface but without the use of a conventional collector [4].

The normal mechanism for collectorless flotation is that of anodic oxidation of the sulphide mineral. Considering a metal sulphide, this is;



The M^{n+} ion usually goes into solution. Its eventual fate depends on the chemistry of the system. It may remain in solution, be complexed, or precipitated. Under certain conditions the sulphur reacts with sulphide to form poly sulphide species;



This reaction is most prominent at pH higher than 8; the concentration of polysulphides at pH 8 is several times greater than that of elemental sulphur. The situation is reversed at pH 6 [21].

Either of the two species, elemental sulphur or the polysulphide, causes the mineral surface to become hydrophobic [22] to a certain degree and this is the basis of collectorless

CHAPTER 1. INTRODUCTION

flotation.

1.1.3. Galvanic interaction:

The flotation of a mineral from a complex mixture is often not consistent with the flotation of the same mineral as a single species. This is due to electrochemical interaction between the two minerals i.e. galvanic interaction [23].

When two minerals or a metal and a mineral are in contact, a galvanic cell is formed. The mineral or metal with the higher rest potential acts as a cathode while the mineral with the lower rest potential is the anode [24].

Among all the sulphide minerals pyrite has the highest rest potential. The mineral may be regarded as electrochemically least active or most cathodic. Electrons flow from a less cathodic mineral to a more cathodic one. Pyrite thus gains electrons (is an electron acceptor), while the less cathodic mineral loses electrons (is an electron donor). One result is the oxidation of sulphide to sulphur on the less cathodic mineral. The formation of elemental sulphur on galena, sphalerite and chalcopyrite has been found to be enhanced in the presence of pyrite at pH 2 [25].

CHAPTER 1. INTRODUCTION

Table 1. Rest potentials of sulphide minerals at pH 4 and 7 [25, 26]

Mineral	Rest potential vs S H E [V]	
	at pH 4	at pH 7
Pyrite	0.66	0.276 to 0.281
Marcasite	0.63	-
Chalcopyrite	0.56	0.189 to 0.195
Sphalerite	0.46	could not be mea
Covellite	0.42	-
Bornite	0.40	-
Galena	0.28	0.142 to 0.195
Argentite	0.28	-
Stibnite	0.12	-
Molybdenite	0.11	-

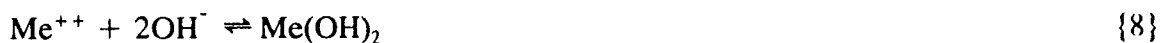
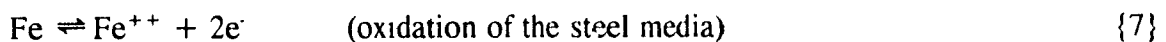
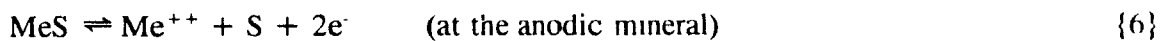
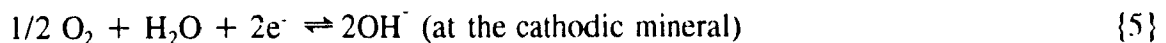
The electrons drawn by pyrite ultimately interact with oxygen present in water forming OH^- ions. One way of hindering the galvanic interaction, therefore, is to increase the pH. Another way is to lower the activity of oxygen in water thus effectively depriving the system of this electron accepting element.

In flotation practice the effect of galvanic interaction has been observed particularly in pyrite flotation [9]. For example, it was found that the flotation of pyrite as a single mineral is not affected by aeration, but when pyrite is in contact with pyrrhotite decreased flotation recovery was observed after aeration. It was explained on the basis of galvanic interaction between the two minerals where electrons are drawn from pyrrhotite to pyrite and transferred

CHAPTER 1. INTRODUCTION

to oxygen. In the absence of aeration galvanic interactions are weakened due to the low activity of oxygen which is the final electron accepting element

Another consequence of galvanic interaction is the effect of grinding media on the floatabilities of sulphide minerals [8, 27, 28]. During grinding an intimate contact is established among the minerals and the grinding media. In complex sulphide ores this leads to multi-electrode galvanic cells. In this type of system the more cathodic of the two minerals (in most cases pyrite) acts as the cathode and grinding media acts as the anode. The second sulphide acts cathodically or anodically depending on its rest potential, and its relative position with respect to the main cathodic and the main anodic minerals. The following reactions occur;



The elemental sulphur formed can cause collectorless flotation and could affect the selectivity of flotation. The deposition of iron hydroxides on a mineral surface generally has an adverse effect on its flotation. The adverse effect of galvanic interactions on flotation can be reduced by using stainless steel as a grinding media instead of mild steel, and introducing

CHAPTER 1. INTRODUCTION

nitrogen to the pulp to decrease the oxygen activity [29, 30] The industrial importance of using nitrogen to get a high grade pyrite concentrate was explored both in the laboratory and in pilot plant by using Noranda minicells [31, 32] Nitrogen flotation of pyrite has also been used for the cleaning of galena, sphalerite and chalcopyrite concentrates [33].

1.2. MINERALS STUDIED

Nickel concentrates from Inco's Sudbury area mills have been processed in the Copper Cliff smelter for over sixty years [34]. Prior to that, Sudbury ores had been smelted directly. Historically, copper-nickel separation from smelter converter matte was achieved by the classical Orford process [35]. A generalized flowsheet of the Copper Cliff Smelter Complex is shown in Figure 1.

Iron sulphide and non-sulphide gangue ("rock") contained in the nickel concentrate are rejected in the smelting-converting process. The molten matte product, typically containing 50% Ni, 25% Cu and 22% S, is cast at about 1000 C, into floor moulds and allowed to slowly cool for four days. During this period heazlewoodite (Ni_3S_2), chalcocite (Cu_2S) and a copper-nickel metallic alloy precipitate and form a coarse grained structure that is amenable to separation by physical means.

A simplified block flowsheet of the Matte Separation Process is shown in Figure 2. Matte ingots, typically weighing 20 tonnes each, are broken and crushed in a three stage crushing plant to approximately minus 1 cm and conveyed to the Matte Separation building. Grinding is carried

CHAPTER 1. INTRODUCTION

out in two parallel circuits each consisting of a rod and ball mill in series producing a flotation feed which is 65% minus 44 μm . Typical throughput of each grinding circuit is 650 tonnes/day. The metallic fraction of the feed is recovered by magnetic separation. This product, containing about 66% Ni, and 15% Cu, is a major component of the feed to the Copper Cliff Nickel Refinery.

The non-magnetic fraction of the matte is fed to flotation. The basis of copper-nickel separation is the selective flotation of chalcocite using diphenylguanidine (DPG) as collector at pH 12.4 (adjusted by saturated lime).

The copper circuit consists of rougher/regrind/two-stage cleaner flotation. Second copper cleaner concentrate typically assays 75% Cu, 3.5% Ni and 21% S and is processed in the copper side of the Copper Cliff Smelter.

The nickel circuit produces two product streams. In the primary circuit, rougher tails is reground and residual chalcocite scavenged to produce a high grade nickel sulphide stream assaying 70% Ni, 0.8% Cu and 26% S. This product is subsequently roasted in fluid bed reactors and the resulting nickel oxide becomes feed for Inco's nickel refinery in Clydach, Wales. A significant amount of the oxide product is also marketed directly, either as is or after chlorination roasting to reduce the copper content even further.

First cleaner tails from the copper circuit and scavenger concentrate from the nickel circuit and scavenger concentrate from the nickel circuit are combined and processed in a middlings circuit which produces the secondary nickel sulphide product. After regrinding, middlings are separated in a rougher/cleaner flotation flowsheet. Middlings rougher tails

CHAPTER 1. INTRODUCTION

represent the low grade nickel sulphide product containing typically 65% Ni, 5.5% Cu and 25% S. This product, after roasting, supplements the feed to the Copper Cliff and Clydach Nickel Refineries. Copper concentrate from the middlings circuit is recycled back to the copper cleaning circuit.

1.3. OBJECTIVES

The general objective of the project was to investigate the electrochemical behaviour of chalcocite (Cu_2S) and heazlewoodite (Ni_3S_2) in the presence and absence of sulfhydryl collectors such as mercaptobenzothiazole and sodium ethyl xanthate using rest potential and cyclic voltammetry measurements. However, a significant amount of Ni dissolution from heazlewoodite was found and this led to a study of the dissolution mechanism of heazlewoodite under different conditions.

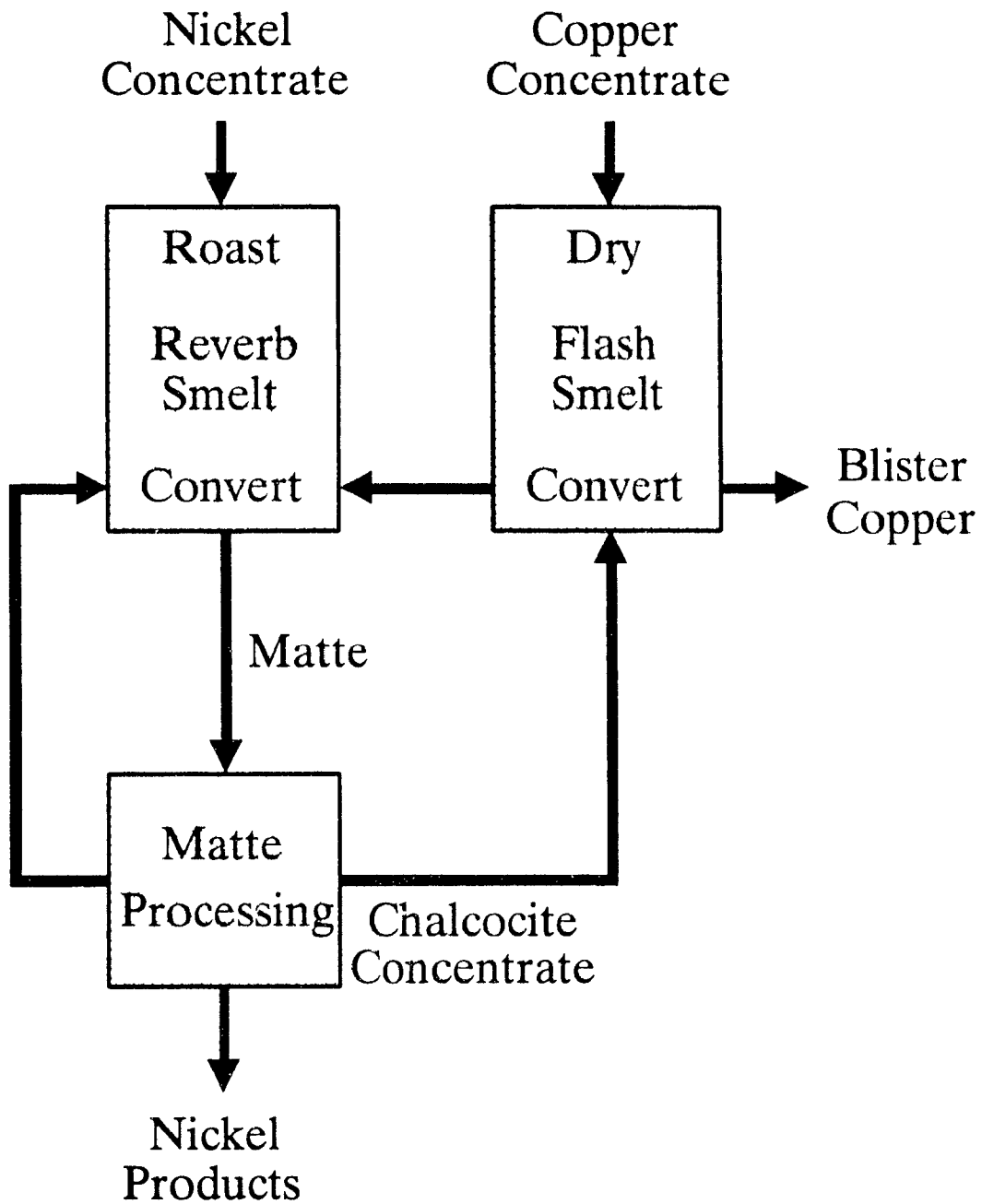


Figure 1. Copper Cliff Smelter

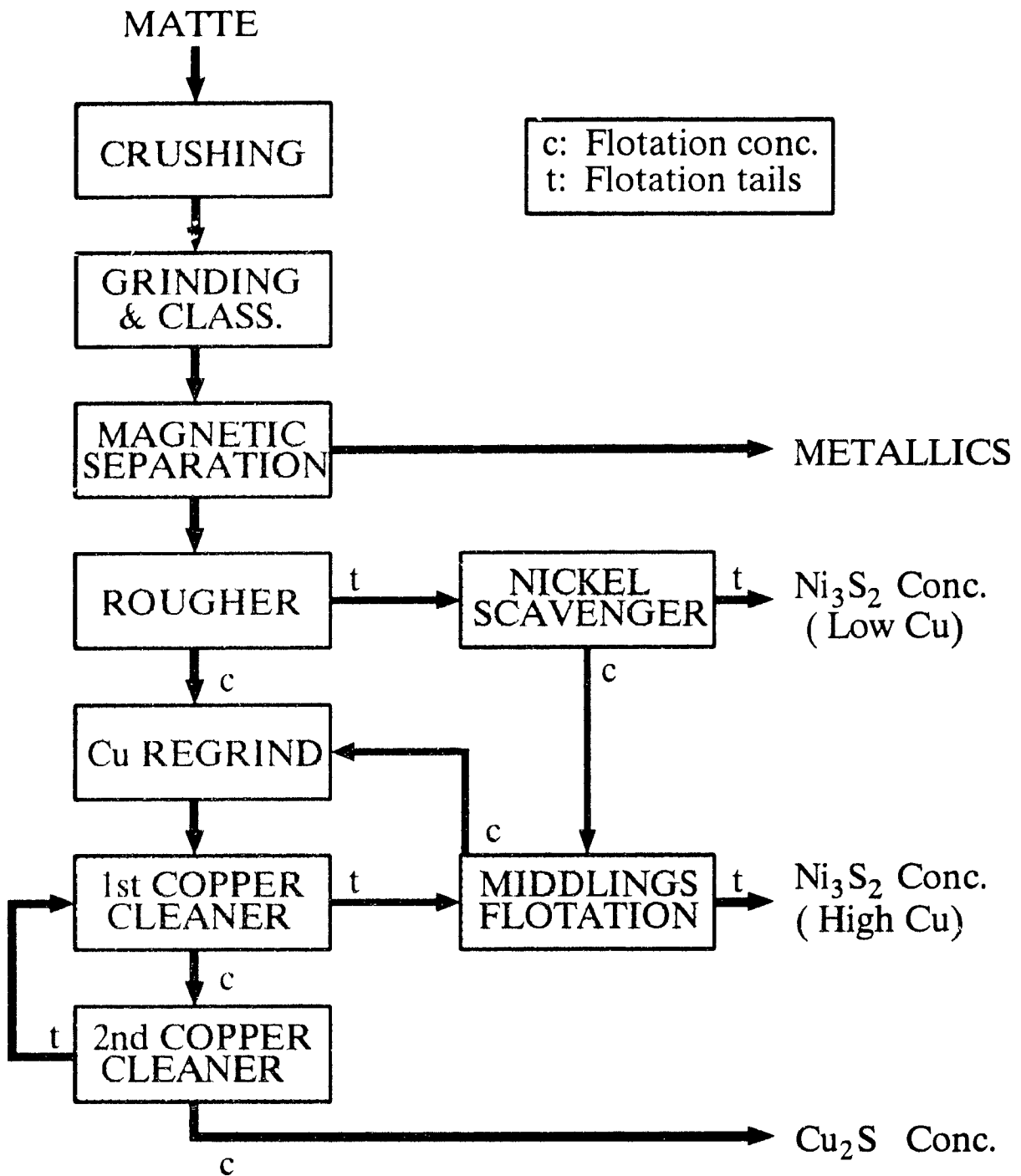


Figure 2. Matte Separation Process

CHAPTER 2. ELECTROCHEMISTRY IN FLOTATION

2.1. FUNDAMENTAL ASPECTS



The electrical potential corresponding to a charge transfer reaction can be measured by setting up an electrochemical cell consisting of two electrodes [36]. One of these electrodes is the working electrode (metal or mineral) in water or a solution containing interacting compounds (e.g., flotation reagents). The second electrode is the reference electrode with a standard electrode potential corresponding to a well defined electrochemical reaction. When there is no current flowing through the cell, the potential of the working electrode eventually reaches a steady state value indicating that the cell is in equilibrium. The potential of the working electrode is then given by the Nerst equation,

$$E = E^{\circ} + \frac{R T}{n F} \ln \frac{C_{\text{Oxd}}}{C_{\text{Red}}} \quad (1)$$

where,

E : Equilibrium potential (Rest potential) (V)

E° : Standard electrode potential (V), it is tabulated for a temperature at 25 °C in chemistry hand book [37].

CHAPTER 2. ELECTROCHEMISTRY IN FLOTATION

n : Number of electrons

R : Gas constant (8 31470 J/deg mole)

T : Temperature ($^{\circ}\text{K}$) ($^{\circ}\text{K} = 273 + ^{\circ}\text{C}$)

F : Faraday constant (96,493.5 J/V equiv)

C_{Red} and C_{Oxd} : Concentrations of Oxd and Red (it is assumed that activity coefficients of Oxd and Red are unity so that concentrations rather than activities may be used in Nerst equation).

For reaction at 25 $^{\circ}\text{C}$,

$$\frac{R T}{n F} \ln \frac{C_{\text{Oxd}}}{C_{\text{Red}}} = \frac{8.3147 \text{ J/}^{\circ}\text{C} \times 298^{\circ}\text{C} \times 2.303}{n \times 96,493.5 \text{ J/V}} \quad (2)$$

$$= \frac{0.059}{n} \log \frac{C_{\text{Oxd}}}{C_{\text{Red}}} \quad (3)$$

and Equation (1) can be rewritten,

$$E = E^{\circ} + \frac{0.059}{n} \log \frac{C_{\text{Oxd}}}{C_{\text{Red}}} \quad (4)$$

As it can be seen from Equation (1), E is a temperature dependent term, meaning it can be defined as a thermodynamic quantity. Therefore, a relation between voltage and standard

CHAPTER 2. ELECTROCHEMISTRY IN FLOTATION

free-energy change [37, 38] is given by,

$$E^{\circ} = - \frac{\Delta G^{\circ}_T}{n F} \quad (5)$$

$$\Delta G^{\circ}_T = \sum \Delta G^{\circ}_P - \sum \Delta G^{\circ}_R \quad (6)$$

where,

ΔG°_T : Free-energy change for reaction

ΔG°_P : Free-energy change for products

ΔG°_R : Free-energy change for reactants

2.2. ELECTROCHEMICAL REACTIONS IN SULPHIDE FLOTATION

In sulphide minerals, sulphur occurs in its lowest oxidation state, -2. Oxidation to the higher oxidation states, 0, +2, +4 and +6, can occur depending upon the activity of the oxidizing agent (e.g. O_2 , Fe^{3+}) in the system. The oxidation occurs by transfer of electrons from sulphur to an electron acceptor. On this principle, a series of charge transfer or electrochemical reactions can be written for the reactions of sulphide minerals in water

In the absence of a flotation reagent the oxidation reaction for any sulphide mineral may

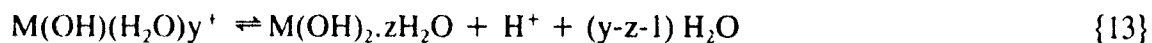
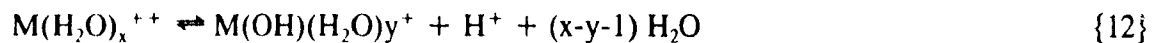
CHAPTER 2. ELECTROCHEMISTRY IN FLOTATION

be represented by,



where M in this case is a divalent ion and S^- is an intermediate product in the oxidation. The metal ions formed by oxidation of sulphide may undergo hydrolysis reactions and/or oxidation.

The following hydrolysis reactions have been suggested [39].



These hydrolysis products may play a significant role in flotation. In particular, some serve as activating species thus promoting the adsorption of collecting agent [40]. The metal ions may be oxidized to higher oxidation states, for instance,



and the oxidized ion may undergo hydrolysis.

The sulphur intermediate (S^-) may undergo oxidation through a series of reactions eventually to form SO_4^{2-} . The first stage of this oxidation process is the formation of elemental

CHAPTER 2. ELECTROCHEMISTRY IN FLOTATION

sulphur,

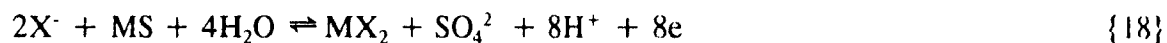
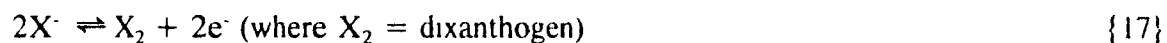


The sulphur formed may nucleate as a new phase or it may be present as a solid solution in the sulphide.

Oxidation of sulphur to sulphonyl species, $S_xO_y^{2-}$, occurs in stages. The formation of these anionic species has been recognized in the adsorption of xanthate ions by exchange adsorption [2].

The interaction of sulphide minerals with flotation reagents, in particular sulphhydryl collectors, also follows an electrochemical mechanism. Some typical examples of electrochemical reactions relevant to sulphide flotation can be summarized as follows:

anodic reactions,



and the cathodic reaction common to all of these is,



Each charge transfer step corresponds to a definite electrochemical potential E related to the Gibbs free-energy change (Equation 5) of the process.

2.3. ELECTRODES

2.3.1. Working electrode

It is at this electrode that the reactions of interest take place. It can be prepared in two ways. One, the packed bed electrode, is prepared by packing mineral particles in a cell with electrical contact being made through a sensing element, usually platinum or gold. The second is the massive mineral electrode, and is prepared by cutting a (pure) crystal of mineral and mounting it in a nonconducting epoxy after making a connection to the mineral surface [26] (Figure 3).

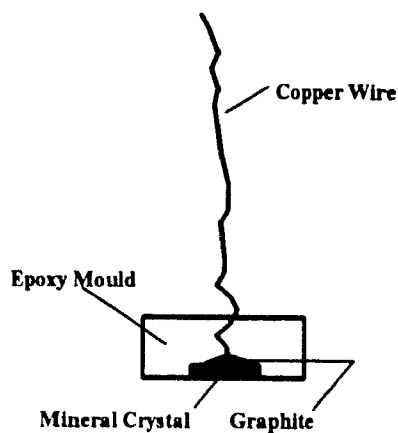


Figure 3. Massive Mineral Electrode

CHAPTER 2. ELECTROCHEMISTRY IN FLOTATION

2.3.2. Counter electrode

The purpose of the counter electrode is to complete the electrical circuit, allow charge to flow through the cell and maintain a constant interfacial potential difference regardless of current. Possible products of reactions at the counter electrode should always be considered, since they may interfere with the reaction being studied [41]. In practice, this interference is prevented by isolating the counter electrode solution from the working electrode maintaining electrical contact via a porous plug (e.g. fritted glass)

2.3.3. Reference electrode

The role of the reference electrode is to provide a fixed potential which does not vary during the experiment. In most cases, it is necessary to relate the potential of the reference electrode to other scales, for example to the standard hydrogen electrode scale. The potential between the working electrode and reference electrode is controlled by a potentiostat. As the reference electrode maintains a fixed potential, any change in applied potential to the cell appears directly across the working electrode-solution interface. The reference electrode serves the dual purpose of providing a thermodynamic reference [42]. The ideal reference electrode is the standard hydrogen electrode (S.H E.) with the reaction,



CHAPTER 2. ELECTROCHEMISTRY IN FLOTATION

The standard electrode potential of this reaction is taken as 0 volt by convention. The measured potential of such a cell directly gives the rest potential of the electrode and is usually denoted by E_h .

It is generally not convenient to set up a cell with a standard hydrogen electrode. Instead, a reference electrode of known rest potential is used. An example is the saturated calomel electrode (S.C.E.). Its redox potential corresponds to the reaction,



with an $E_h = 0.247$ volt.

By using S.C.E., the potential of the cell thus measured is the potential of the mineral electrode with respect to S.C.E. In order to obtain the value of E_h , the E_h value of the S.C.E. is added to the measured cell potential, i.e. in general,

$$E_{h(\text{mineral})} = E_{(\text{measured})} + E_{h(\text{reference})} \quad (7)$$

2.4. CYCLIC VOLTAMMETRY

In practice the potential of a mineral is not always the equilibrium value because the mineral reacts with the reagent components at different rates. In order to study such a dynamic state it is necessary to follow the changes occurring when the potential of the electrode varies.

CHAPTER 2. ELECTROCHEMISTRY IN FLOTATION

This is accomplished by imposing a potential on the electrode by an external power source. When this is done electric current flows through the electrode which is no longer in a state of equilibrium. (At equilibrium, the net current flow is zero)

Measurement of the current at the working electrode under applied potential from an external source provides information on electrode reactions. The technique is called cyclic voltammetry. The experimental curve showing the variation of current with applied potential is called a voltammogram. At specific potentials a notable current flow occurs and this indicates a charge transfer reaction between the electrode and the solution. This reaction can be either anodic (oxidation) or cathodic (reduction). When it takes place in the anodic region, the reaction is called an anodic reaction and vice versa [43].

The basic equipment for cyclic voltammetry is a potentiostat. It is available in different models. The one assembled at McGill is the Princeton Applied Research, PAR 273 model with Head Start 1.3 software which enables the user to follow the current as a function of applied potential over any desired range. The electrochemical cell designs for packed bed and massive electrodes are shown in Figure 4. The mineral acts as the working electrode. The platinum wire acts as the counter electrode. A potential is applied to the working electrode from an external power source and potential with respect to S.C.E is recorded. The schematic representation of the system is shown in Figure 5 [44].

To illustrate the type of results obtained and their analysis, consider the Fe(II)-Fe(III) reaction. Figure 6 shows the voltammogram of 0.2 M FeSO₄ at pH 2.5.

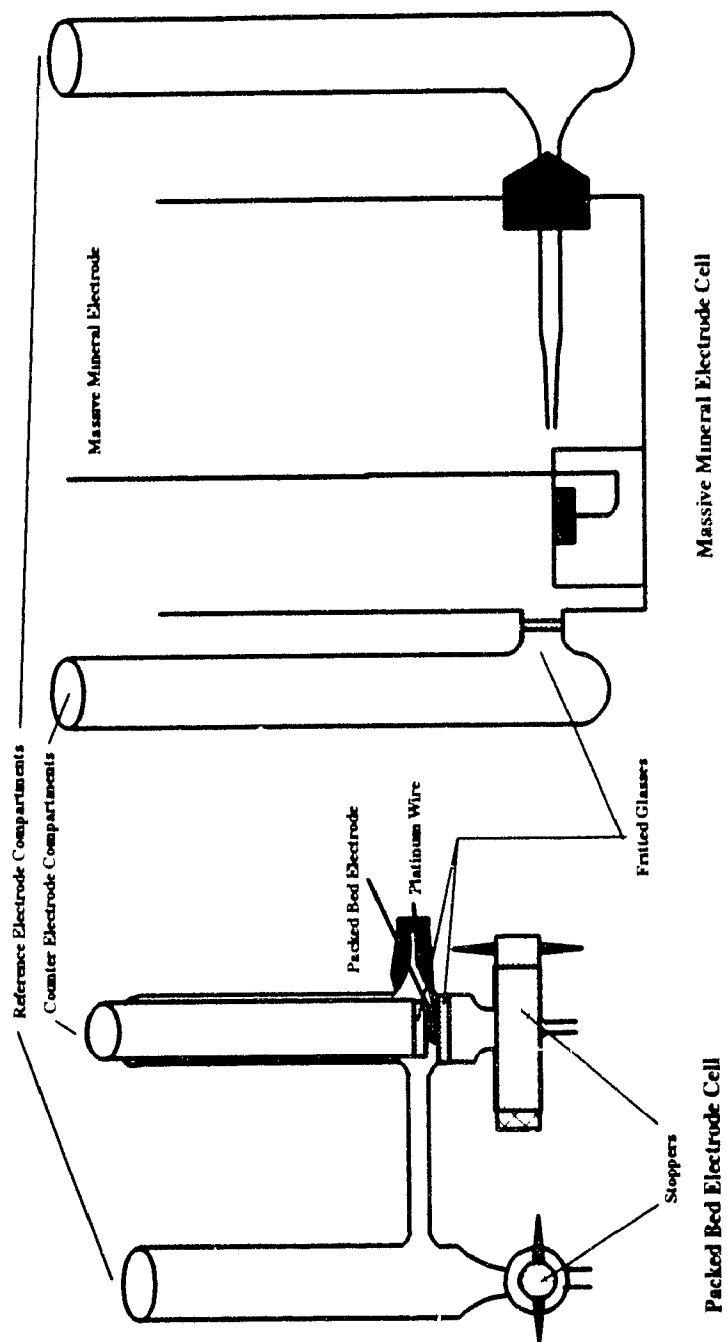


Figure 4. Electrochemical Cells

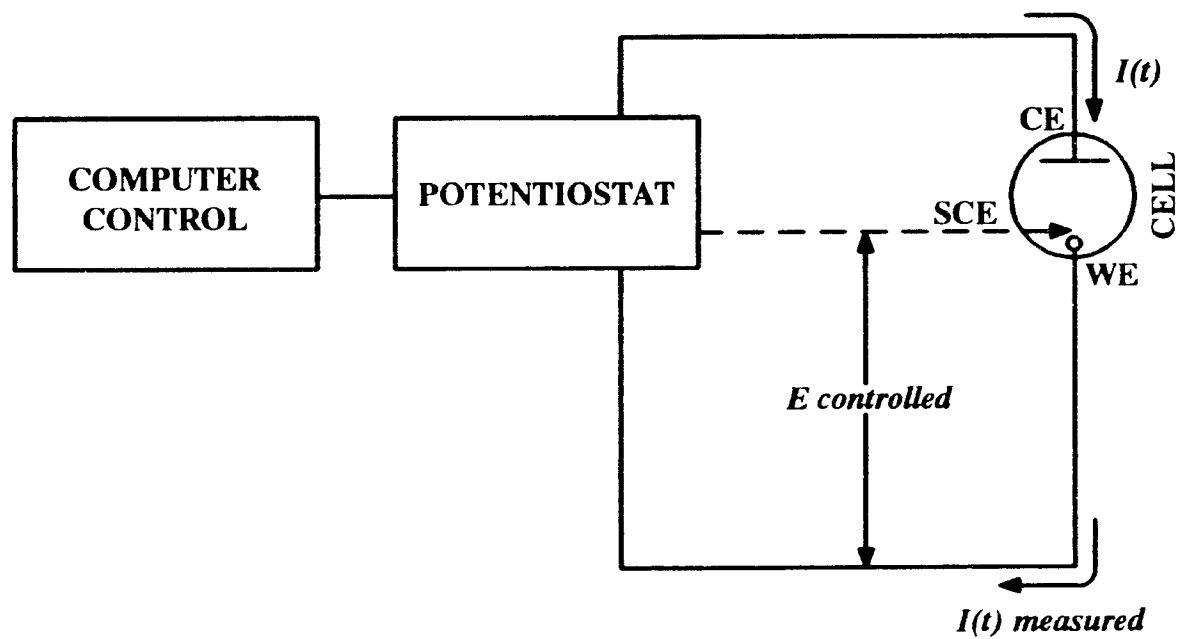


Figure 5. Schematic Representation of Potentiostat Measurement System.

SCE Standard Calomel Electrode (reference)

CE Counter Electrode

WE Working Electrode (mineral)

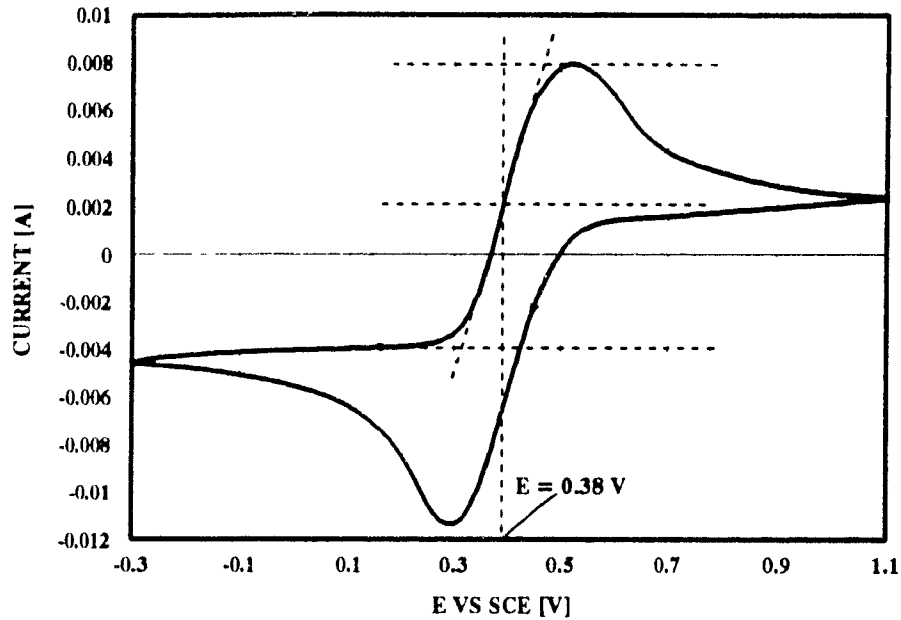
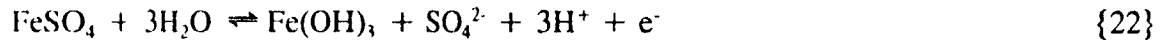


Figure 6. 0.2 M Ferrous Sulphate at pH 2.5.

As can be seen, the voltammogram shows a charge transfer reaction at ≈ 0.38 V (vs. S.C.E.), or at ≈ 0.63 V vs. S.H.E.. Assuming the following redox reaction,



then the corresponding potential can be calculated by the following steps: First, the free-energy changes of FeSO_4 , H_2O , Fe(OH)_3 and SO_4^{2-} , are found [38], namely -829.7, -237.2, -694.5 and -741.9 kJ, respectively. Second, the free-energy change of reaction (ΔG_T°) is calculated using Equation (6),

$$\Delta G_T^\circ = (-694.5 + -741.9) - (-829.7 + (-3) \times -237.2) = 104.9 \text{ kJ} \quad (8)$$

CHAPTER 2. ELECTROCHEMISTRY IN FLOTATION

Then third, the standard potential of the reaction (E°) is calculated by using Equation (5),

$$E^{\circ} = \frac{104.9}{1 \times 96,5} = 1.09 \text{ V} \quad (9)$$

Using Equation (4) the redox potential (E) of the reaction is calculated,

$$E = 1.09 + \frac{0.0592}{1} \log [SO_4^{2-}] [H^+]^3 \quad (10)$$

According to Equation (10) E is equal to 0.65 V. The voltammogram reading value 0.63 V and the calculated value 0.65 V are comparable.

The same procedure for estimating the potential illustrated in Figure 6 was used in all subsequent cases.

2.5. REVIEW OF CHALCOCITE-HEAZLEWOODITE SYSTEM

Chalcocite-water and chalcocite-water-xanthate reactions have been studied using electrochemical and flotation techniques by a number of investigators [45-55]. In water, two anodic peaks were observed at potentials of -0.35 and 0.25 V (vs S.H.E). Electrochemical reactions converting HS^- to S^0 [53] and Cu_2S to Cu^0 [55] have been suggested for the first anodic peak. The combination of two reactions, oxidation of Cu_2S to Cu^{++} and hydrolysis of Cu^{++} to

CHAPTER 2. ELECTROCHEMISTRY IN FLOTATION

$\text{Cu}(\text{OH})_2$, have been suggested for the second anodic peak [56, 57]. In the presence of xanthate, five distinct interactions have been recognized at potentials of -0.3, -0.16, -0.09, -0.05 and 0.25 V by Mielczarski et al. [46, 47]. They suggested that the first peak corresponded to the oxidation of hydrosulfide ions, that the second and third were the underpotential deposition of xanthate, and that the fourth and fifth were the formation of bulk copper xanthate and other cuprous sulfide oxidation products. Another series of electrochemical measurements were conducted by Walker et al. [50]. They found four distinct interactions which they ascribed to: (1) a reaction of EtX to form ethylperxanthate at reducing potentials near -0.255 V (all the potentials are respect to SHE); (2) a reaction of EtX with soluble Cu^{++} forming CuEtX at 0.217 V, (3) an exchange reaction with EtX displacing an oxidation product; and (4) a charge transfer oxidation reaction. The exchange and charge transfer reactions occurred over the potential range -0.255 to 0.145 V and formed cuprous and possibly cupric xanthates as adsorbed hydrophobic species.

Electrochemical studies on the heazlewoodite-xanthate system have been described by Critchley and Hunter [58]. Their investigations have provided information on charge transfer reactions of heazlewoodite in water and in xanthate solutions. In water they found a large anodic peak corresponding to the oxidation of Ni_3S_2 to Ni^{++} and also, probably, to the formation of elemental sulphur on the surface. This effect was suppressed at pH 11.5, probably due to the formation of nickel hydroxy species. In the presence of xanthate, dixanthogen and NiETX_2 were the major products at around 0.295 V and 0.055 V respectively. The formation of an unidentified product was also observed at -0.055 V from UV spectra of surface leachates.

CHAPTER 3. EXPERIMENTAL PROCEDURE AND RESULTS

3.1. DISSOLUTION:

Preliminary experiments showed significant Ni dissolution from heazlewoodite (and matte). It was considered important to follow this up prior to main objective of the electrochemical study.

Experiment 1: Fifteen grams of freshly ground -150+200 mesh matte were slurred in 500 ml buffer solutions [59] at pH 8, 10 and 12. The slurry was stirred by a mechanical stirrer at constant speed and air exposure. Samples were drawn at 15, 30, 60, 120, 180 and 360 minutes. The Ni and Cu concentrations were analyzed for each experiment by atomic absorption spectroscopy. The results are shown in Table 2 and Figures 7 and 8

Table 2. Dissolution of matte at different pH

Time [min]	Concentration pH 8 [ppm]		Concentration pH 10 [ppm]		Concentration pH 12 [ppm]	
	Ni	Cu	Ni	Cu	Ni	Cu
15	2.40	0.80	0.15	0.30	0.00	0.00
30	3.25	0.85	0.15	0.30	0.00	0.10
60	3.90	1.00	0.15	0.40	0.00	0.20
120	5.60	0.90	0.15	0.40	0.00	0.20
180	6.00	0.80	0.15	0.50	0.00	0.25
360	8.10	0.85	0.25	0.30	0.00	0.15

Experiment 2: Experiment 1 was repeated with fifteen grams of freshly ground -150+200 mesh heazlewoodite and chalcocite. The results are shown in Table 3 and Figures 9 and 10. A

CHAPTER 3. EXPERIMENTAL PROCEDURE AND RESULTS

comparison of dissolution between heazlewoodite and chalcocite is shown in Figure 11.

Table 3. Dissolution of heazlewoodite and chalcocite at different pH

Time [min]	Concentration pH 8 [ppm]		Concentration pH 10 [ppm]		Concentration pH 12 [ppm]	
	Ni	Cu	Ni	Cu	Ni	Cu
15	9.6	0.80	0.05	0.60	0.00	0.25
30	14.3	0.85	0.05	0.50	0.00	0.30
60	20.5	1.05	0.05	0.65	0.00	0.30
120	25.9	1.00	0.10	0.65	0.00	0.35
180	28.7	1.20	0.25	0.65	0.00	0.40
360	32.1	1.25	0.40	0.60	0.00	0.35

Experiment 3: Using the general procedure of Experiment 1, fifteen grams of heazlewoodite were slurried in 500 ml buffer solution of pH 8 and the effect of air, nitrogen, and oxygen was studied. The results are shown in Table 4 and Figure 12.

Table 4. Dissolution of heazlewoodite at pH 8

Time [min]	Ni Concentration [ppm]		
	Air	Oxygen	Nitrogen
15	9.6	10.5	10.9
30	14.3	14.5	15.0
60	20.5	21.3	21.0
120	25.9	28.7	29.0
180	28.7	32.1	30.0
360	32.1	36.6	29.5

CHAPTER 3. EXPERIMENTAL PROCEDURE AND RESULTS

Experiment 4: To further study the dissolution, Experiment 2 was repeated in the presence of ethylenediaminetetraacetic acid (EDTA) (5g/kg sample) at pH 8. The results are shown in Table 5 and Figure 13.

Table 5. Dissolution of heazlewoodite in presence and absence of EDTA at pH 8

Time [min]	Ni Concentration [ppm]	
	No EDTA	With EDTA
15	9.6	27.2
30	14.3	33.6
60	20.5	39.9
120	25.9	44.0
180	28.7	46.1
360	32.1	48.3

CHAPTER 3. EXPERIMENTAL PROCEDURE AND RESULTS

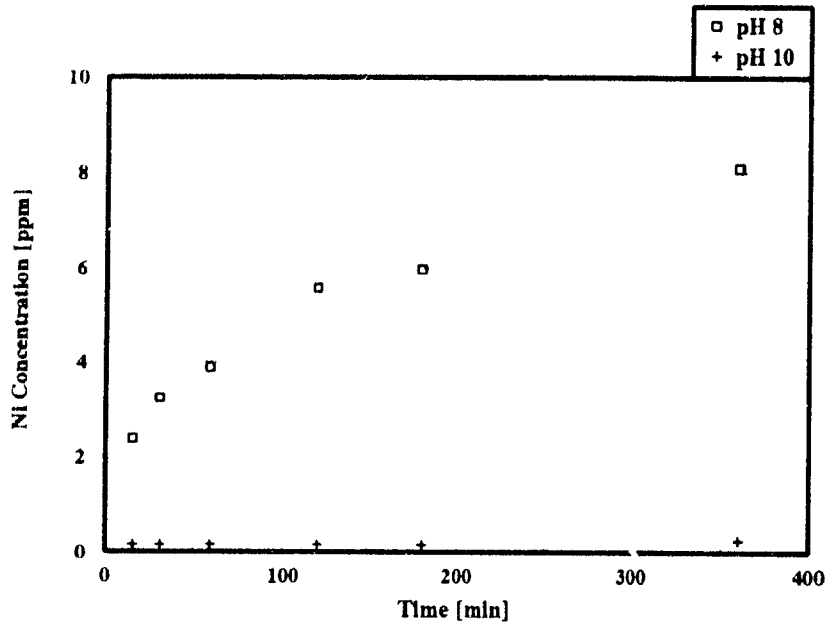


FIGURE 7. Ni Dissolution from matte at different pH.

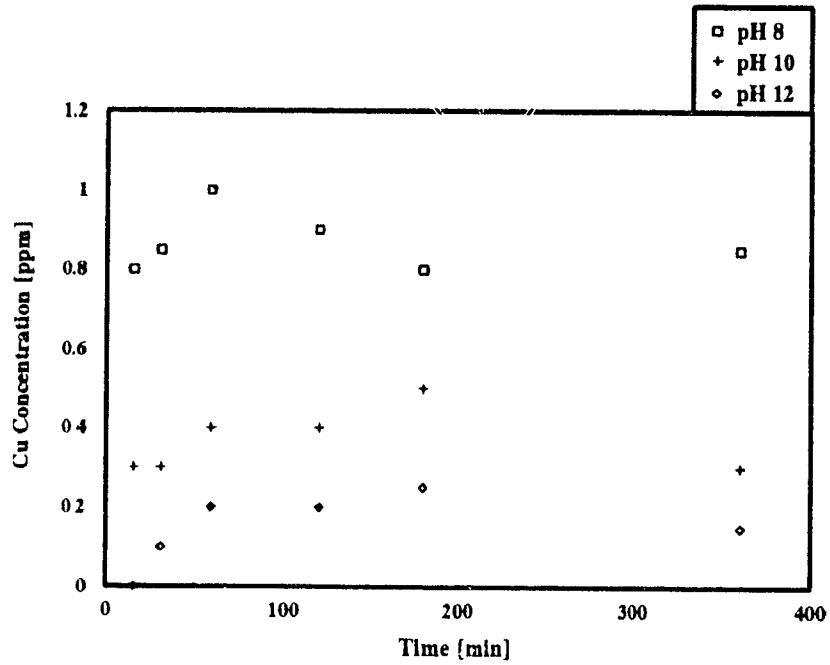


FIGURE 8. Cu Dissolution from matte at different pH.

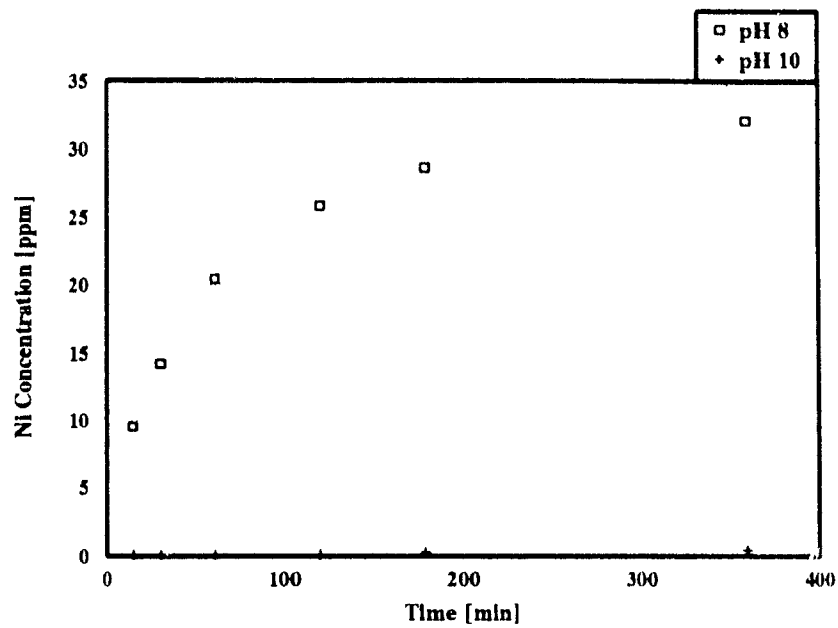


FIGURE 9. Ni Dissolution from heazlewoodite at different pH.

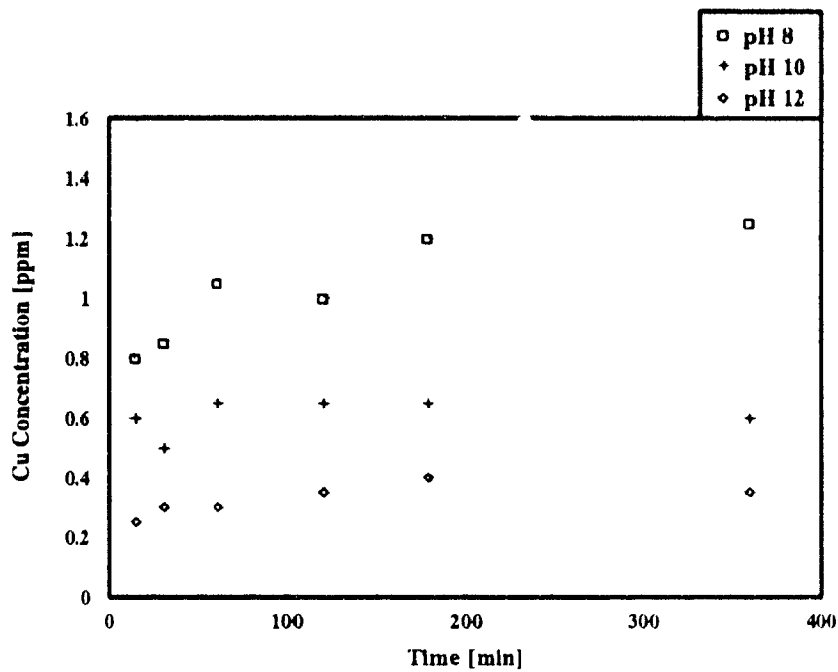


FIGURE 10. Cu Dissolution from chalcocite at different pH.

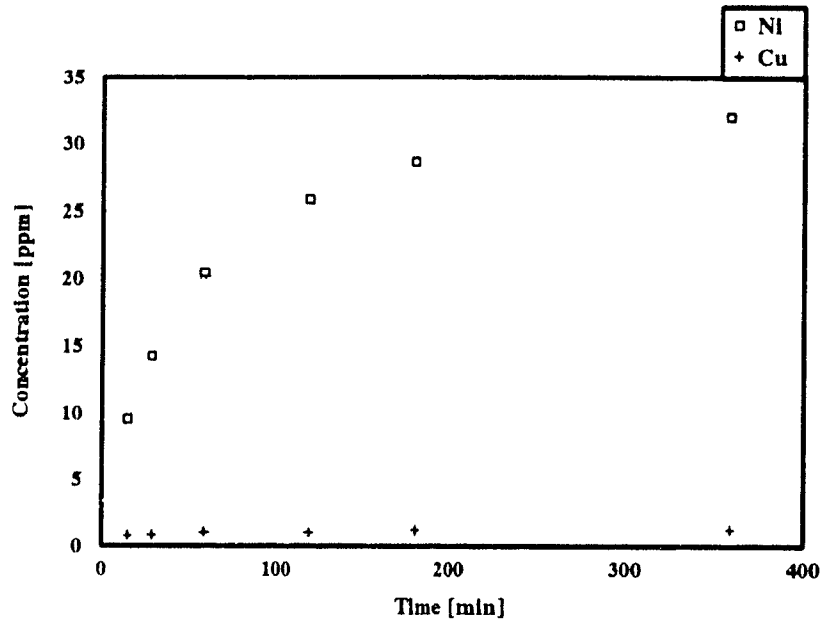


FIGURE 11. Dissolution of chalcocite and heazlewoodite at pH 8.

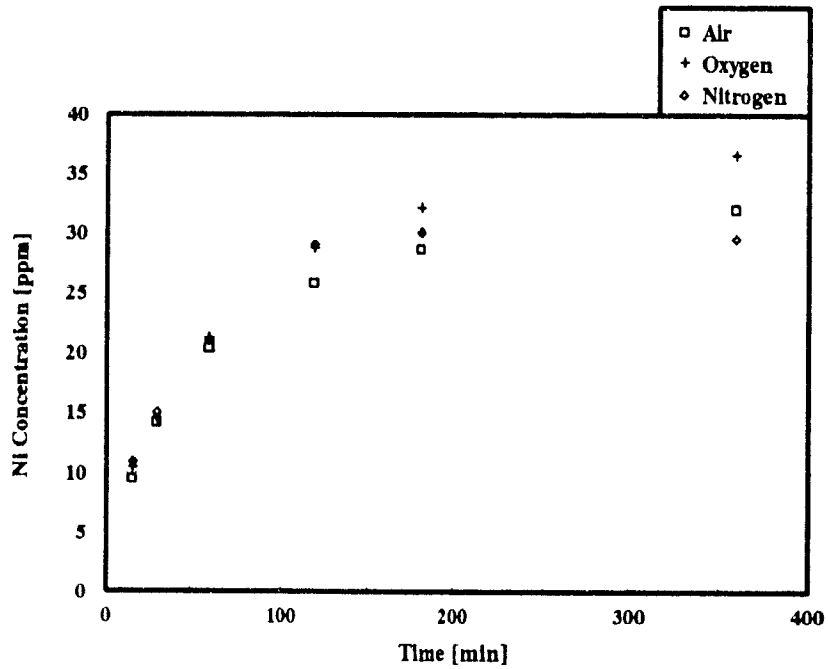


FIGURE 12. Dissolution of heazlewoodite at pH 8 in different conditions.

CHAPTER 3. EXPERIMENTAL PROCEDURE AND RESULTS

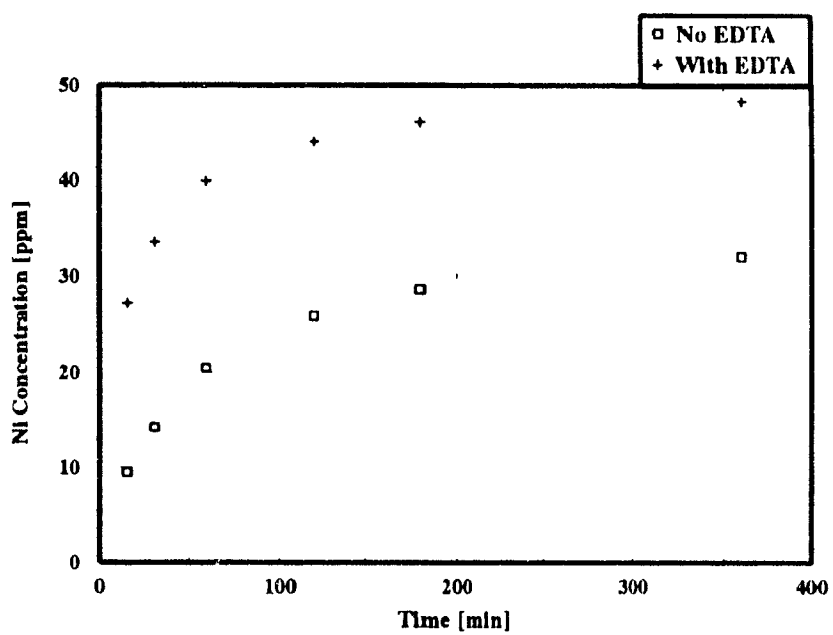


FIGURE 13. Dissolution of heazlewoodite at pH 8.

CHAPTER 3. EXPERIMENTAL PROCEDURE AND RESULTS

3.2. REST POTENTIAL:

Experiment 1: Rest potential measurements were performed for chalcocite and heazlewoodite in buffer solutions of pH 4, 6, 8, 9.3, 10 and 12. Also, rest potentials of chalcocite were measured with respect to a heazlewoodite electrode and compared with the calculated value. The results are shown in Table 6 and Figures 14 and 15.

Table 6. Rest potential values of chalcocite and heazlewoodite

pH	Rest Potential Values (± 30 mV)			
	Chalcocite E_h [V]	Heazlewoodite E_h [V]	Measured $E_{(Ch-Lz)}$ [V]	Calculated $E_{h(Ch)} - E_{h(Lz)}$ [V]
4	0.30	-0.05	0.32	0.35
6	0.28	-0.08	0.33	0.36
8	0.24	0.03	0.20	0.21
9.3	0.21	0.12	0.05	0.09
10	0.18	0.11	0.03	0.07
12	0.09	0.07	0.01	0.02

$E_{(Ch-Lz)}$ Rest potential of chalcocite with respect to heazlewoodite electrode.

Experiment 2: Rest potential measurements of chalcocite and heazlewoodite were performed in the presence and absence of 2×10^{-3} M sodium ethyl xanthate and mercaptobenzothiazole. The results are shown in Table 7 with a comparison of the rest potentials for each mineral in water alone. The results are also shown in Figures 16-19.

CHAPTER 3. EXPERIMENTAL PROCEDURE AND RESULTS

Table 7. Rest potential values of chalcocite and heazlewoodite in the presence and absence of collectors

pH	Rest Potential Values (± 30 mV)					
	In Water		In 2×10^{-3} M NaEX		In 2×10^{-3} M MBT	
	Chalcocite E_h [V]	Heazlewoodite E_h [V]	Chalcocite E_h [V]	Heazlewoodite E_h [V]	Chalcocite E_h [V]	Heazlewoodite E_h [V]
4	0.30	-0.05	0.14	-0.03	0.15	0.01
6	0.28	-0.08	0.09	-0.02	0.11	0.03
8	0.24	0.03	0.01	0.01	-0.01	0.07
9.3	0.21	0.12	-0.07	0.06	0.01	0.1
10	0.18	0.11	-0.07	0.07	0.01	0.1
12	0.09	0.07	-0.08	0.05	0.01	0.04

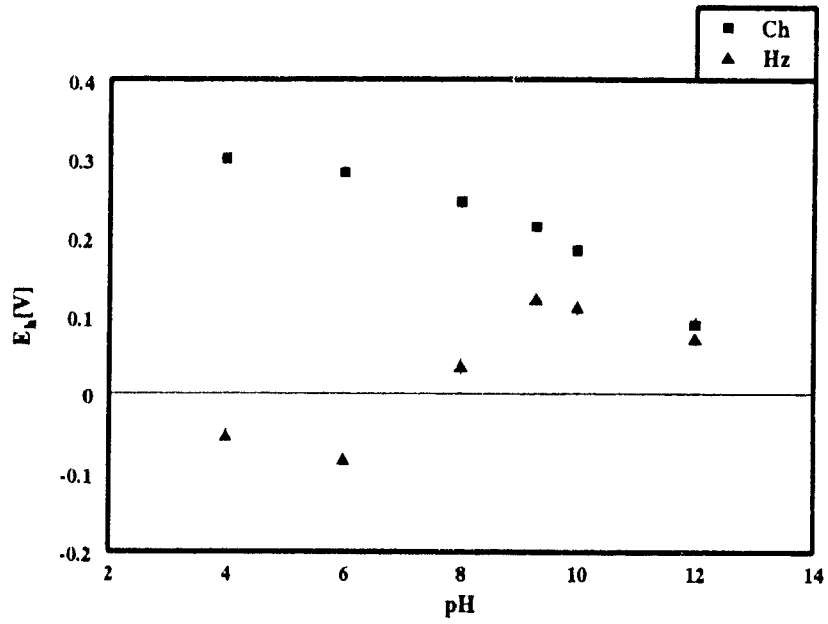


FIGURE 14. Rest potentials of chalcocite and heazlewoodite at different pH.

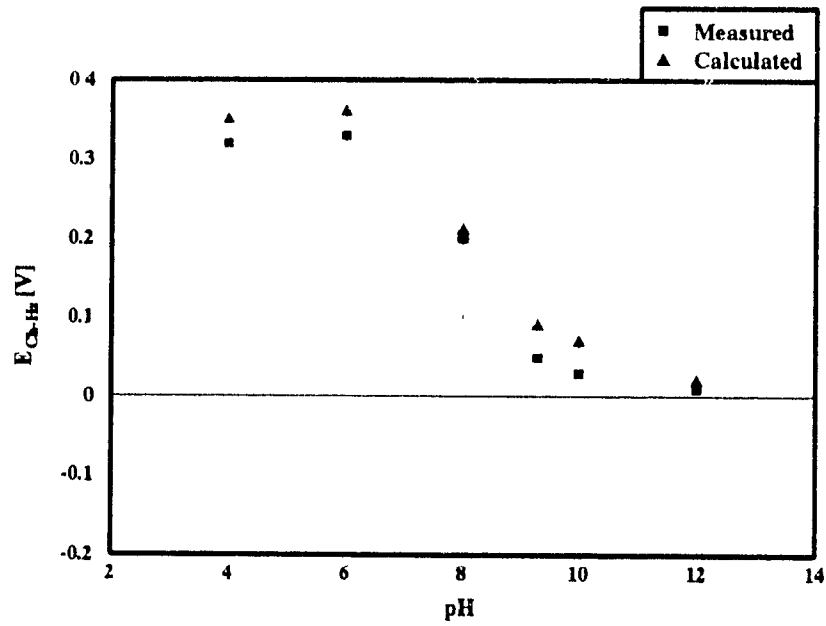


FIGURE 15. Rest potential of chalcocite relative to heazlewoodite electrode at different pH.

CHAPTER 3. EXPERIMENTAL PROCEDURE AND RESULTS

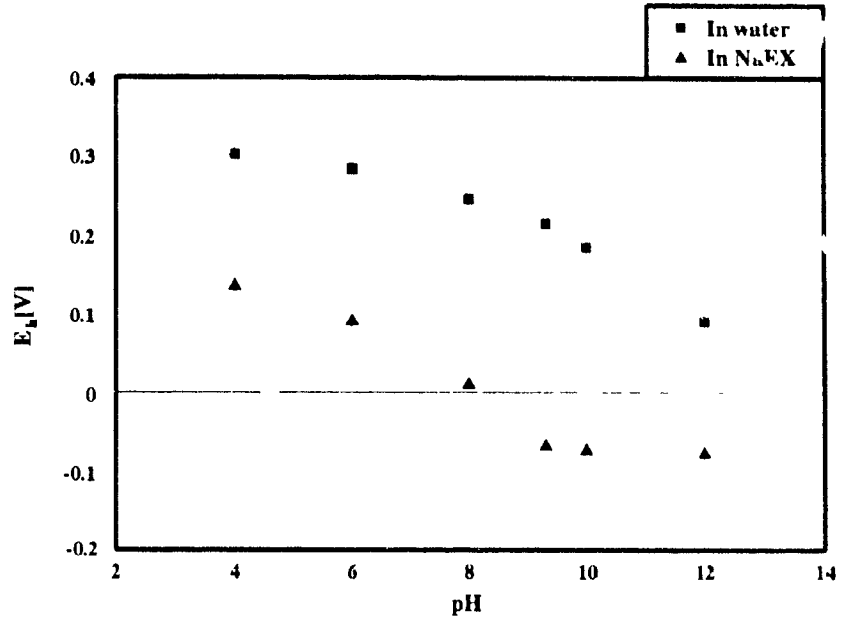


FIGURE 16. Rest potentials of chalcocite at different pH.

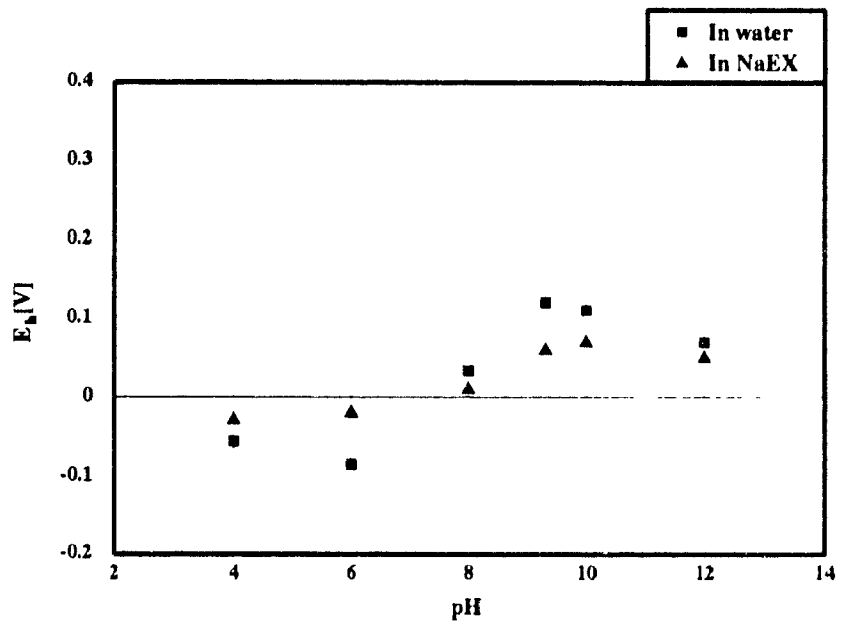


FIGURE 17. Rest potentials of heazlewoodite at different pH.

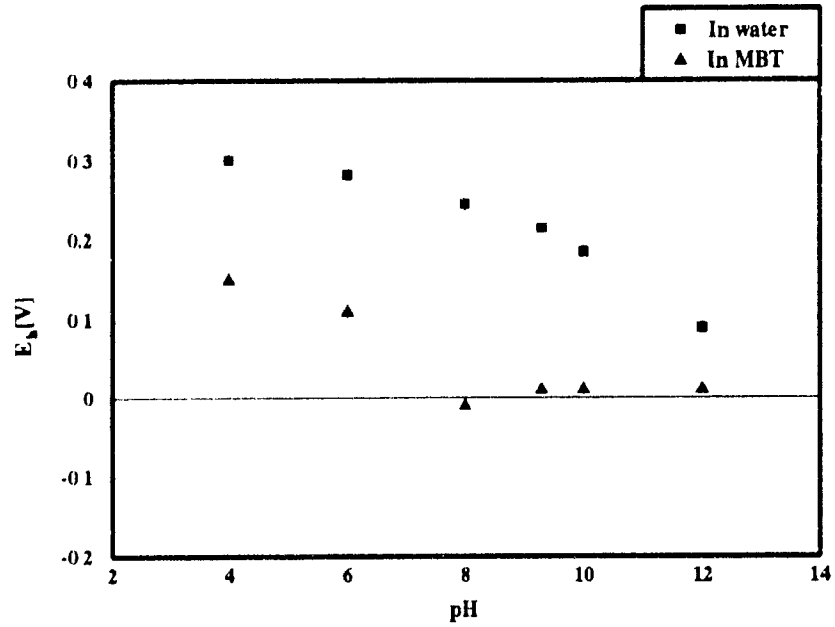


FIGURE 18. Rest potentials of chalcocite at different pH.

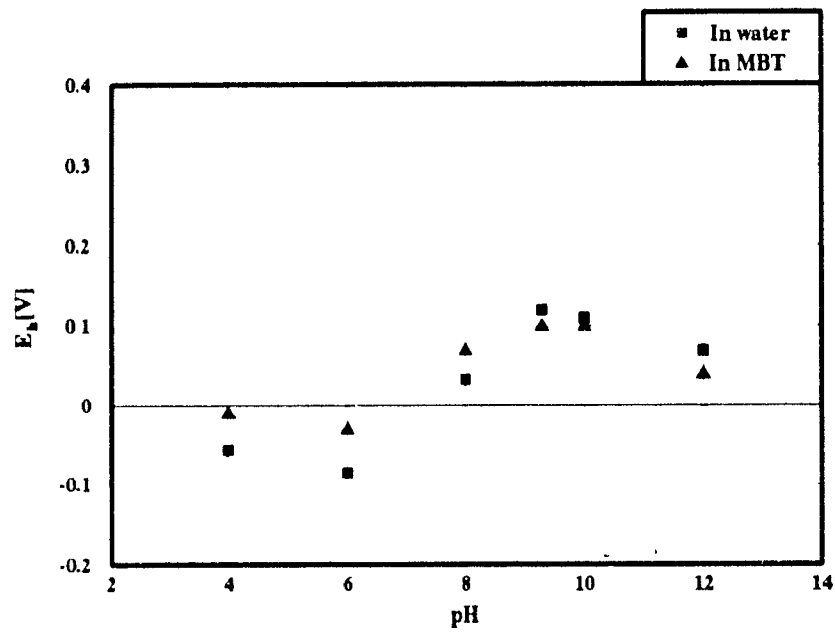


FIGURE 19. Rest potentials of heazlewoodite at different pH.

CHAPTER 3. EXPERIMENTAL PROCEDURE AND RESULTS

3.3. CYCLIC VOLTAMMETRY:

Cyclic voltammetric measurements were performed using an EG & G Princeton Applied Research Potentiostat/Galvanostat Model 273 with the Head-Start software. A standard three electrode electrochemical cell was used. Experiments were performed with chalcocite and heazlewoodite massive electrodes in the absence and presence of collectors. Collector strength was 2×10^{-3} M and pH was 10 and 12. In the case of chalcocite, to compare with available literature data, pH 9.3 was also used [53]. For the purposes of comparison the same potential interval was applied to heazlewoodite (Figures 20 and 21). The electrodes were polished before each experiment on 6 μ m abrasive ethanol solution on a 6 μ m polisher head after which the electrode immersed in ethanol solution followed by immersion in pH 2 HCl solution and rinsed with distilled water [60]. The results of the cyclic voltammetric measurements are shown in Figures 20 to 30. All the potential values in the text are with respect to standard hydrogen electrode (0.0 V).

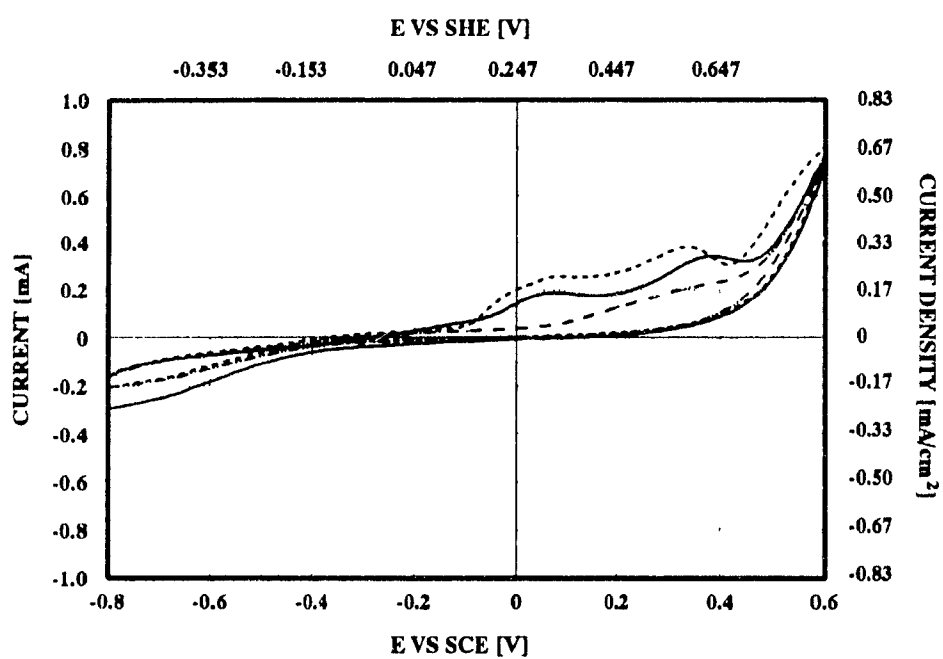


FIGURE 20. Heazlewoodite massive electrode at pH 10.

- In water
- - - In NaEX
- . - . In MBT

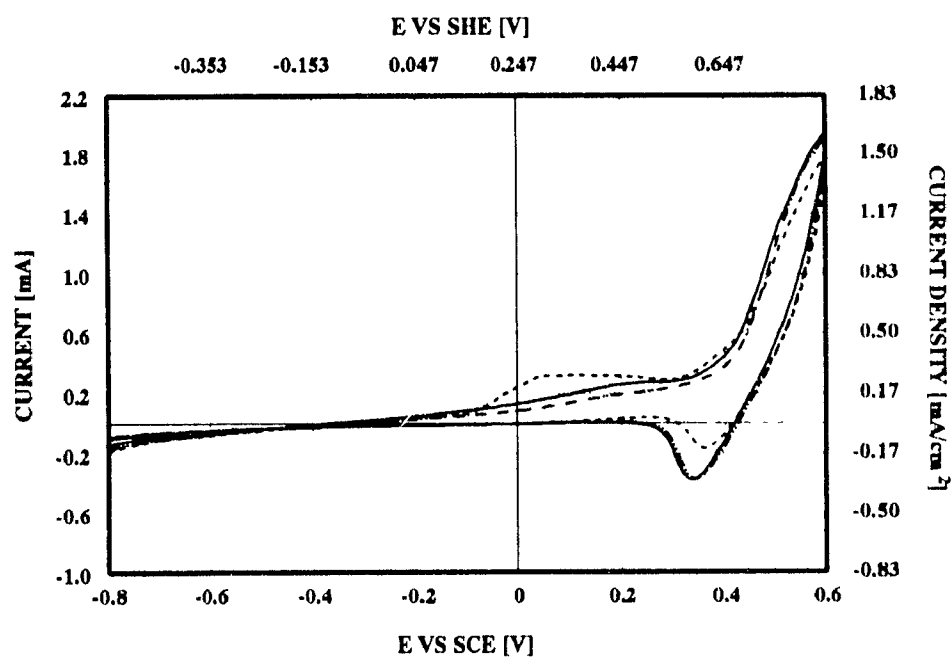


FIGURE 21. Heazlewoodite massive electrode at pH 12.

- In water
- - - In NaEX
- · - In MBT

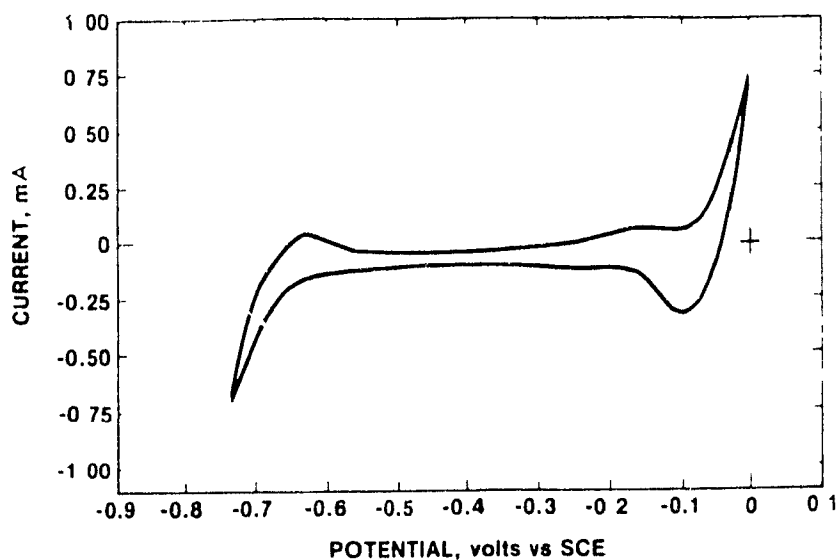


FIGURE 22. Voltammogram of single particle chalcocite electrode at pH 9.3. (By Walker et al. (1984)).

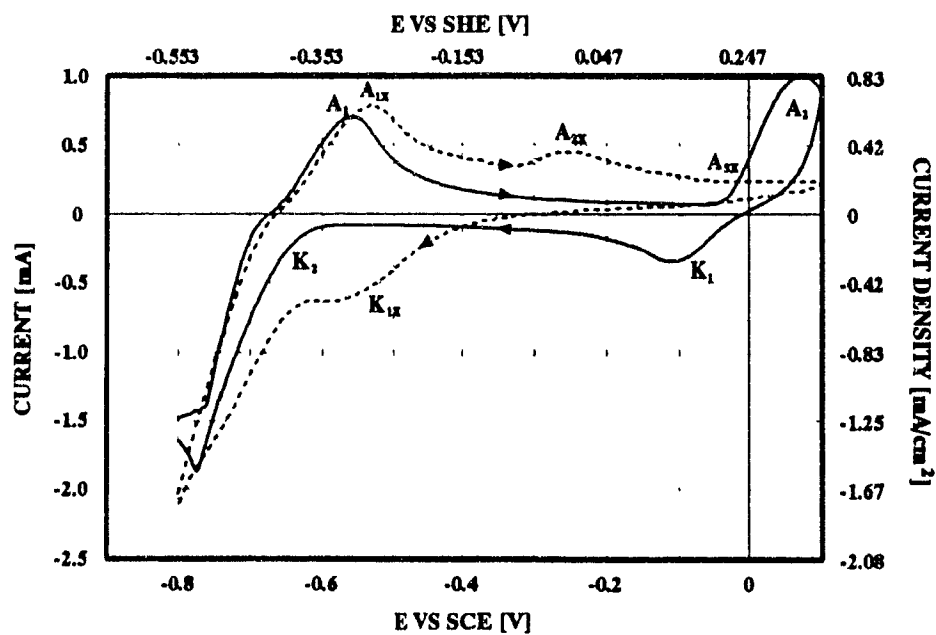


FIGURE 23. — Chalcocite massive electrode at pH 9.3 (0.05 M sodium borate).
 --- Chalcocite massive electrode at pH 9.3 in the presence of 2×10^{-3} M NaEX.

CHAPTER 3. EXPERIMENTAL PROCEDURE AND RESULTS

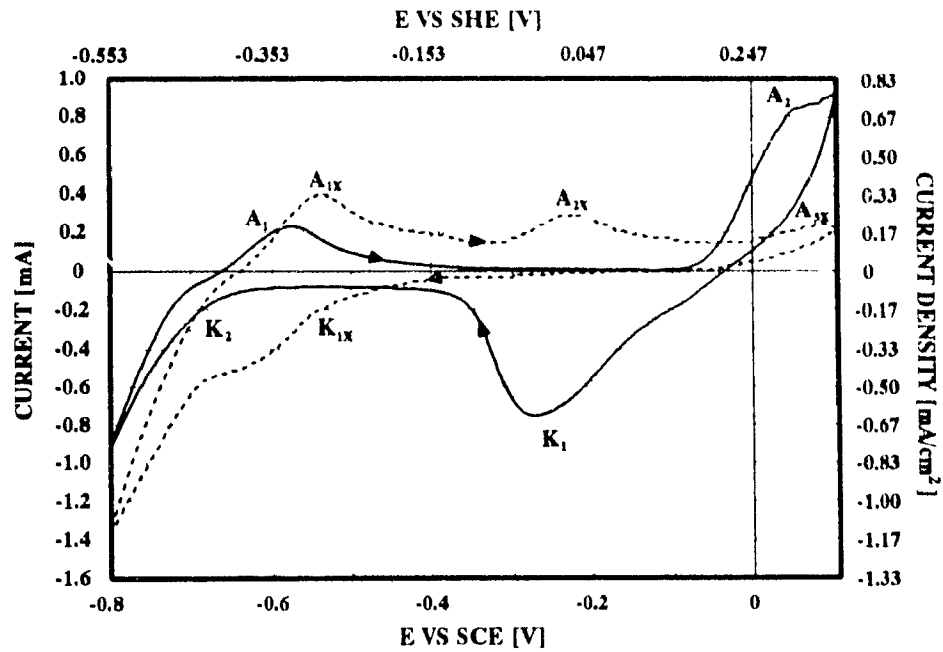


FIGURE 24. — Chalcocite massive electrode at pH 10.
 --- Chalcocite massive electrode at pH 10 in the presence of $2 \times 10^{-3} \text{ M NaEX}$.

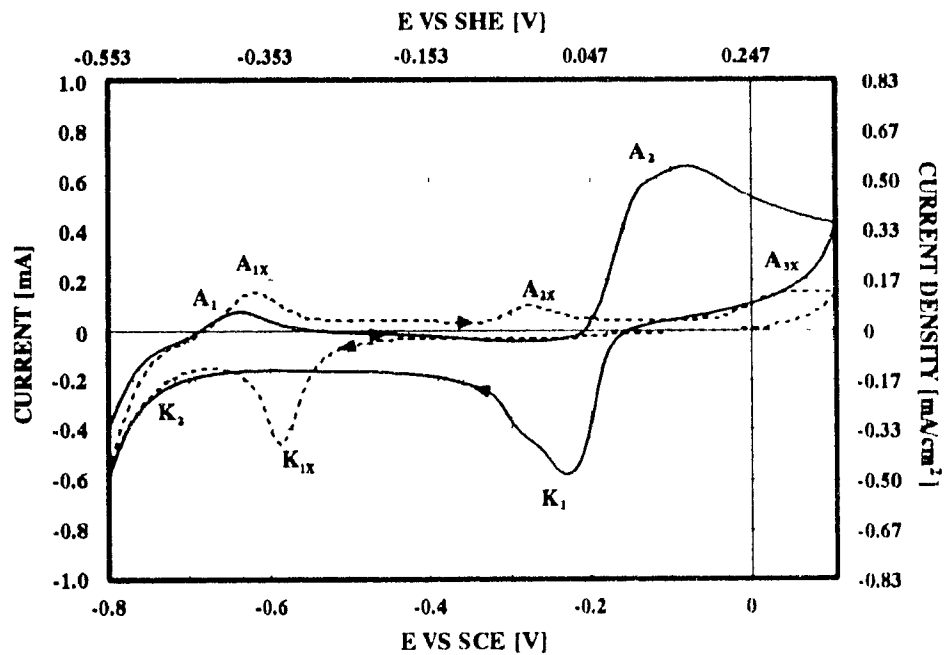


FIGURE 25. — Chalcocite massive electrode at pH 12.
 --- Chalcocite massive electrode at pH 12 in the presence of $2 \times 10^{-3} \text{ M NaEX}$.

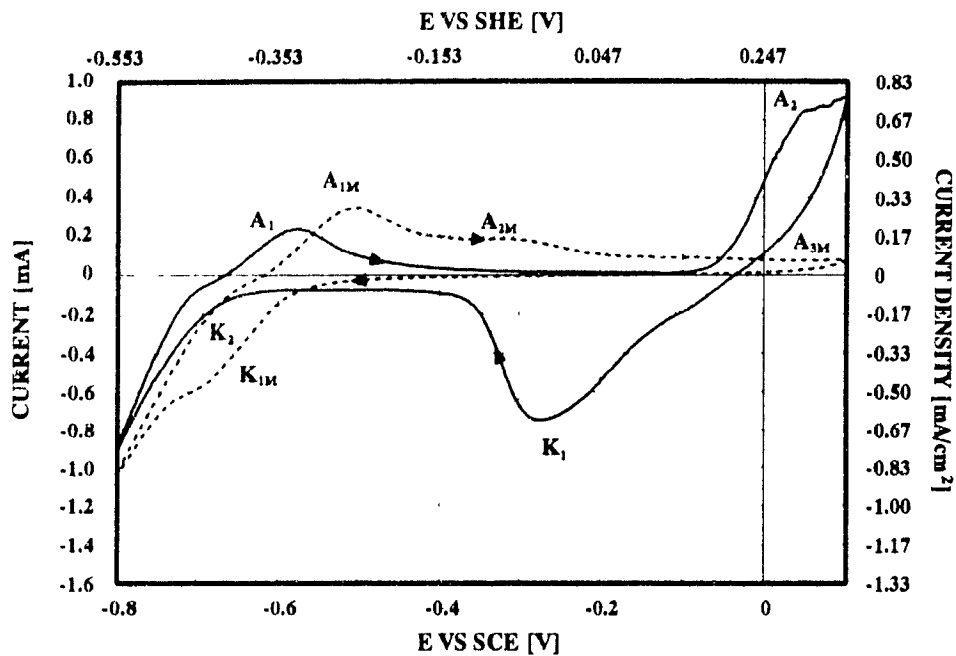


FIGURE 26. — Chalcocite massive electrode at pH 10.
 - - - Chalcocite massive electrode at pH 10 in the presence of $2 \times 10^{-3} \text{ M MBT}$.

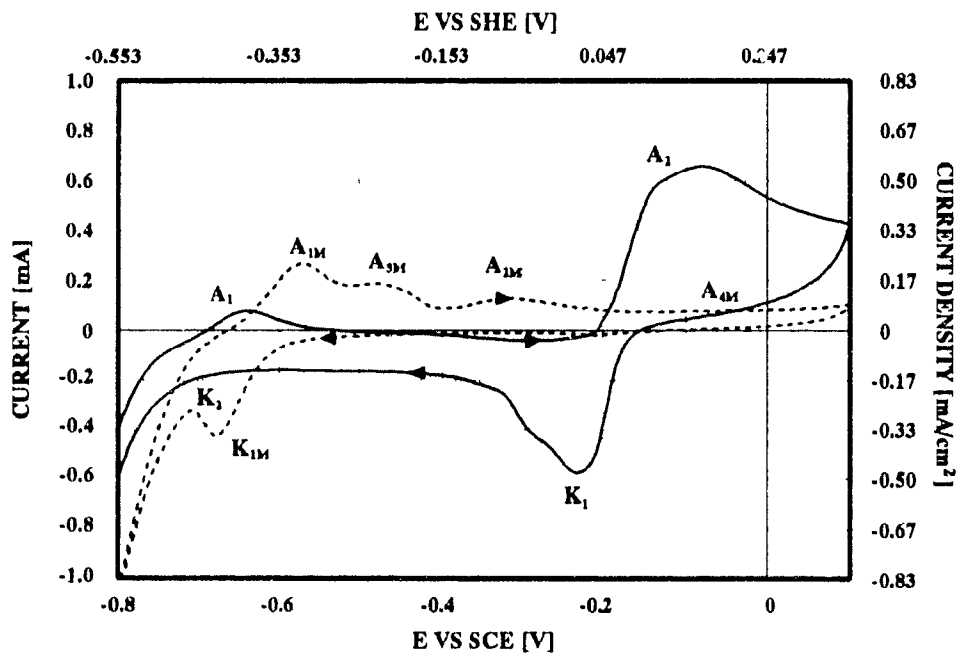


FIGURE 27. — Chalcocite massive electrode at pH 12.
 - - - Chalcocite massive electrode at pH 12 in the presence of $2 \times 10^{-3} \text{ M MBT}$.

CHAPTER 3. EXPERIMENTAL PROCEDURE AND RESULTS

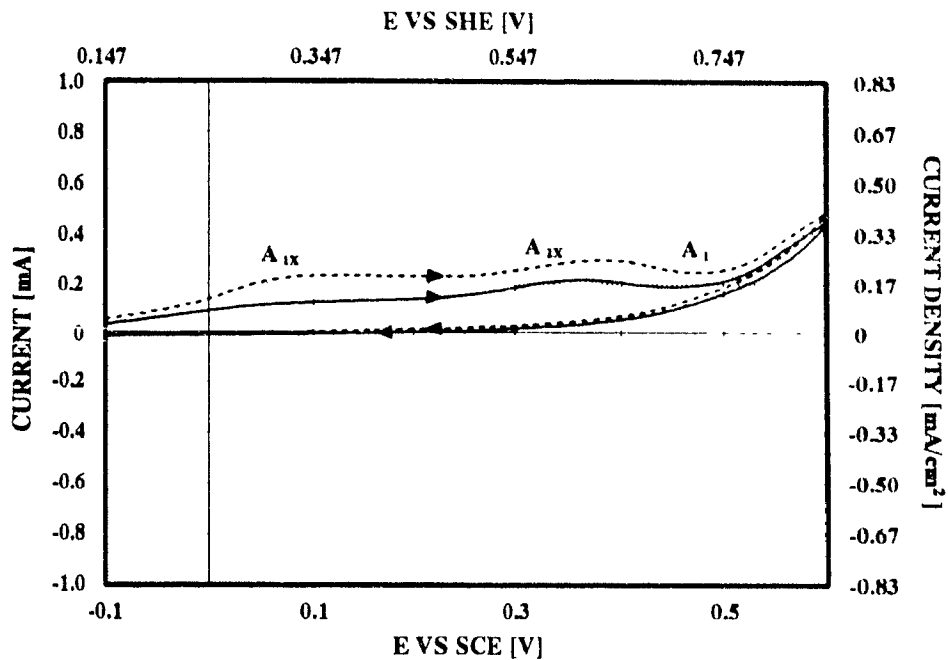


FIGURE 28. — Heazlewoodite massive electrode at pH 10.
 --- Heazlewoodite massive electrode at pH 10 in the presence of $2 \times 10^{-3} \text{ M NaEX}$.

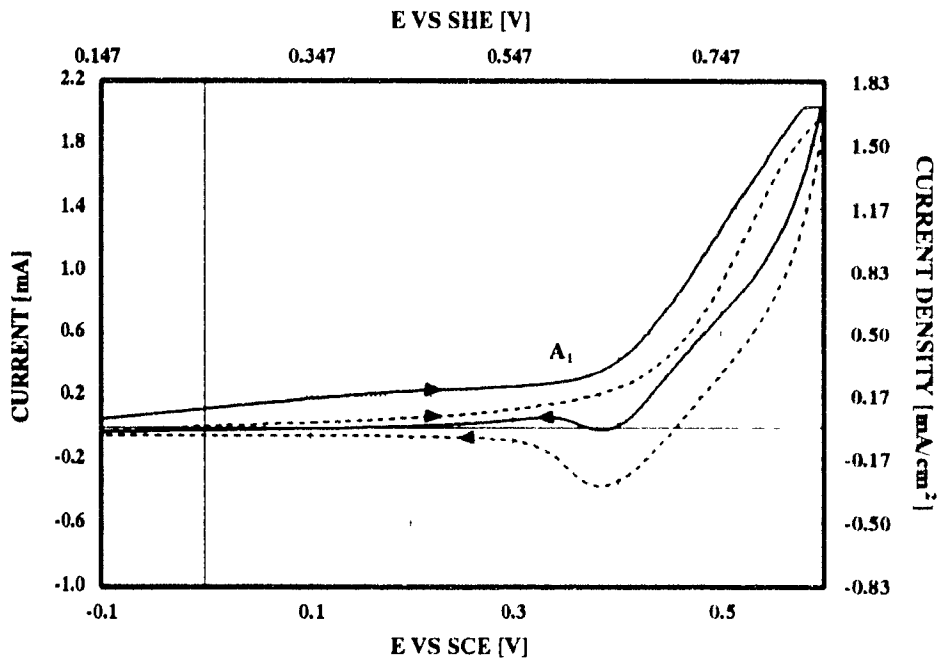


FIGURE 29. — Heazlewoodite massive electrode at pH 12.
 --- Heazlewoodite massive electrode at pH 12 in the presence of $2 \times 10^{-3} \text{ M NaEX}$.

CHAPTER 3. EXPERIMENTAL PROCEDURE AND RESULTS

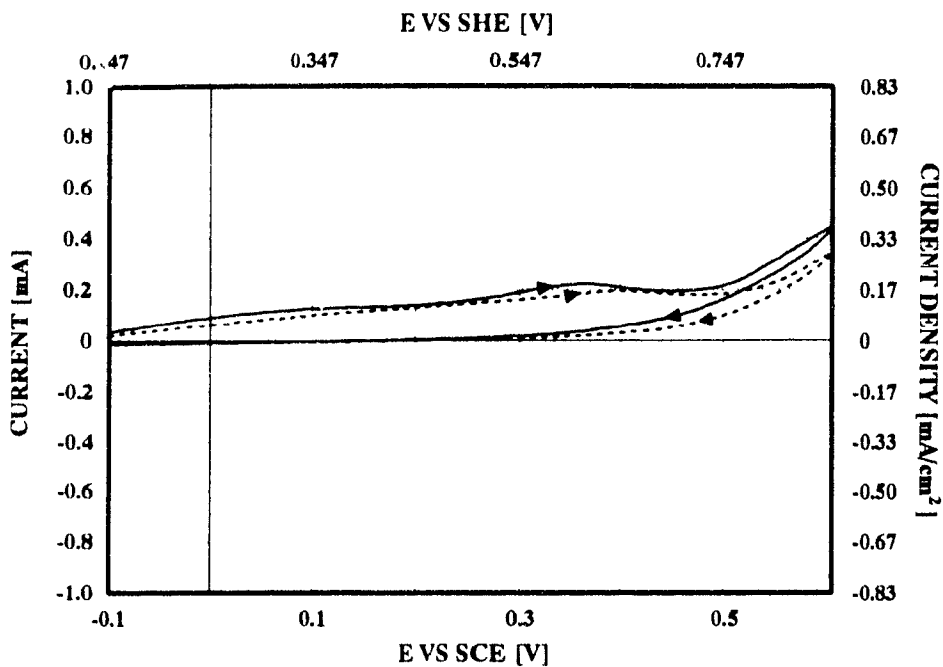


FIGURE 30. — Heazlewoodite massive electrode at pH 10.
 --- Heazlewoodite massive electrode at pH 10 in the presence of 2×10^{-3} M MBT.

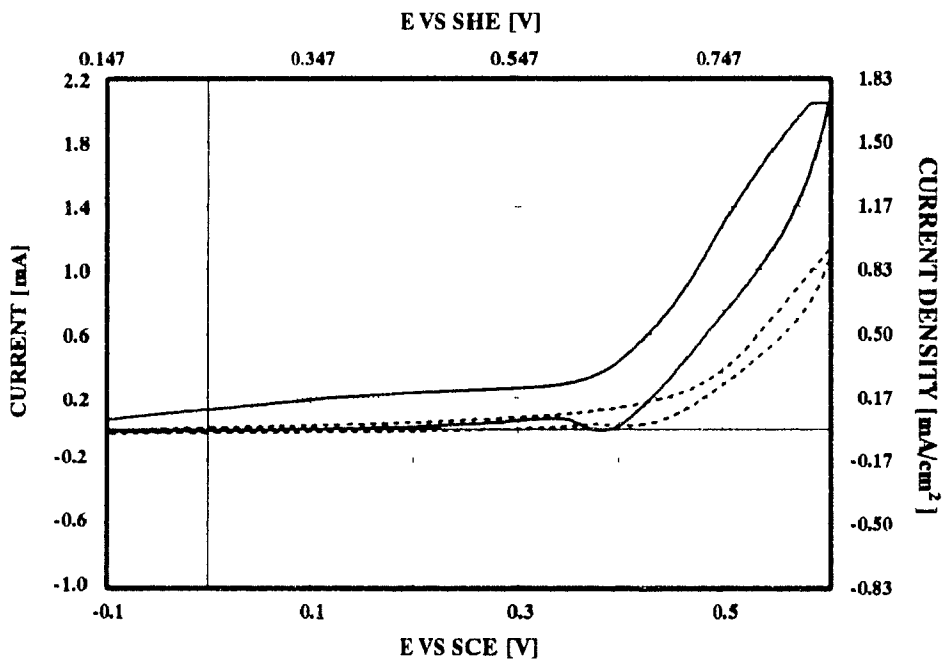


FIGURE 31. — Heazlewoodite massive electrode at pH 12.
 --- Heazlewoodite massive electrode at pH 12 in the presence of 2×10^{-3} M MBT.

CHAPTER 3. EXPERIMENTAL PROCEDURE AND RESULTS

3.4. CONTACT ANGLE:

Contact angles were measured using a captive-bubble apparatus [61] (Figure 32) equipped with a three-electrode electrochemical cell constructed with two parallel plate windows. The electrode surface was cleaned prior to each measurement by using same method as described in cyclic voltammetry experiments. After pre-reduction at -0.55 V, the potential was stepped to more positive values, held for 5 minutes at each value, and the contact angle measured by a goniometer. Each bubble was deposited on the surface by using a $500\ \mu\text{m}$ threaded plunger syringe (Fisher Sci.). The average of three measurements was taken at each condition. The contact angle measurements were performed in the presence and absence of 2×10^{-3} M NaEX pH values 10 and 12. The contact angle as a function of potential is shown in Figures 33 and 34. The comparison between contact angle and cyclic voltammograms are shown in Figures 35 and 36.

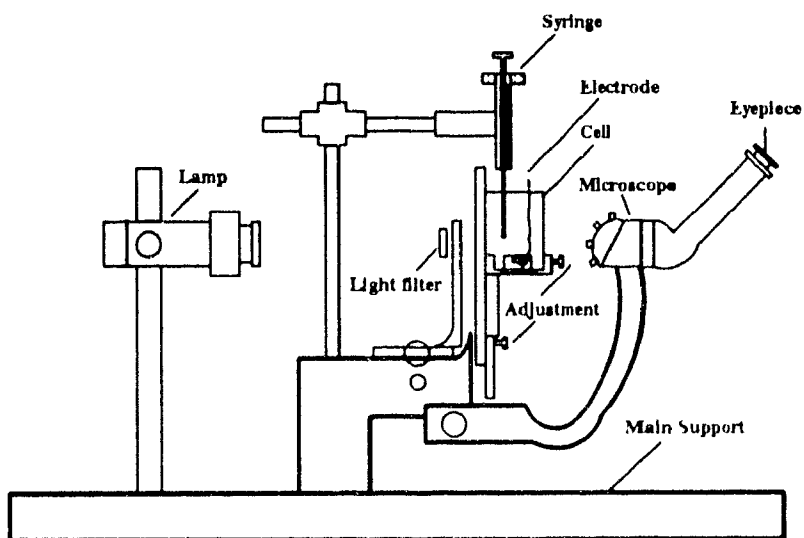


FIGURE 32. A schematic representation of the captive-bubble contact angle apparatus.

CHAPTER 3. EXPERIMENTAL PROCEDURE AND RESULTS

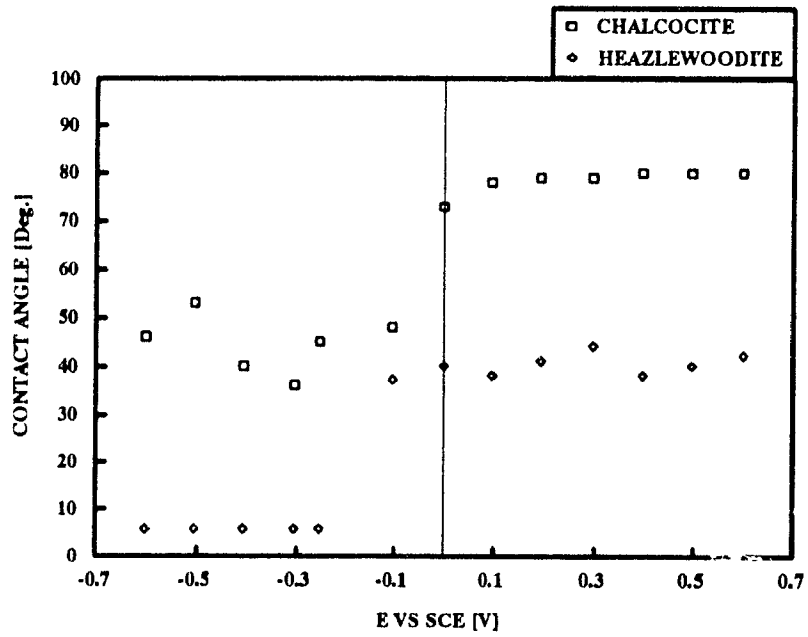


FIGURE 33. Contact angle values of chalcocite and heazlewoodite at pH 10 in the presence of 2×10^{-3} M NaEX.

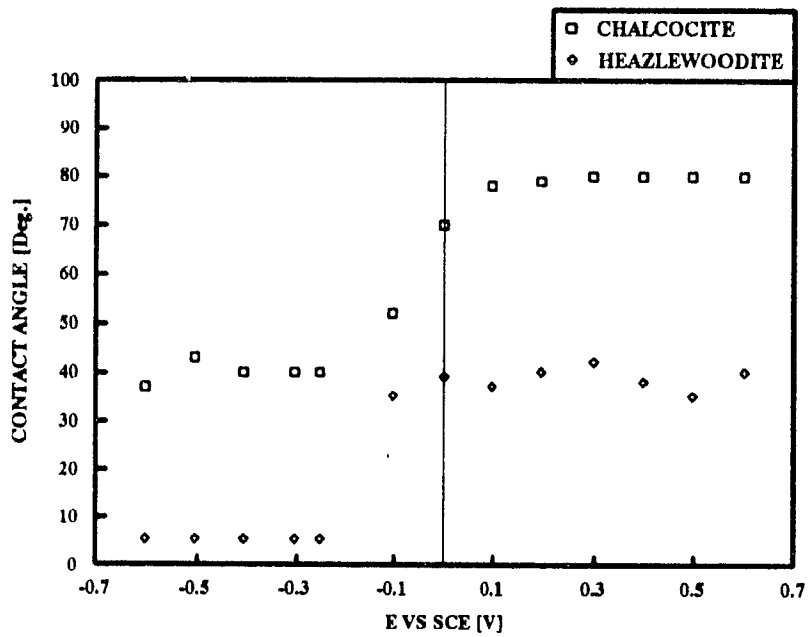


FIGURE 34. Contact angle values of chalcocite and heazlewoodite at pH 12 in the presence of 2×10^{-3} M NaEX.

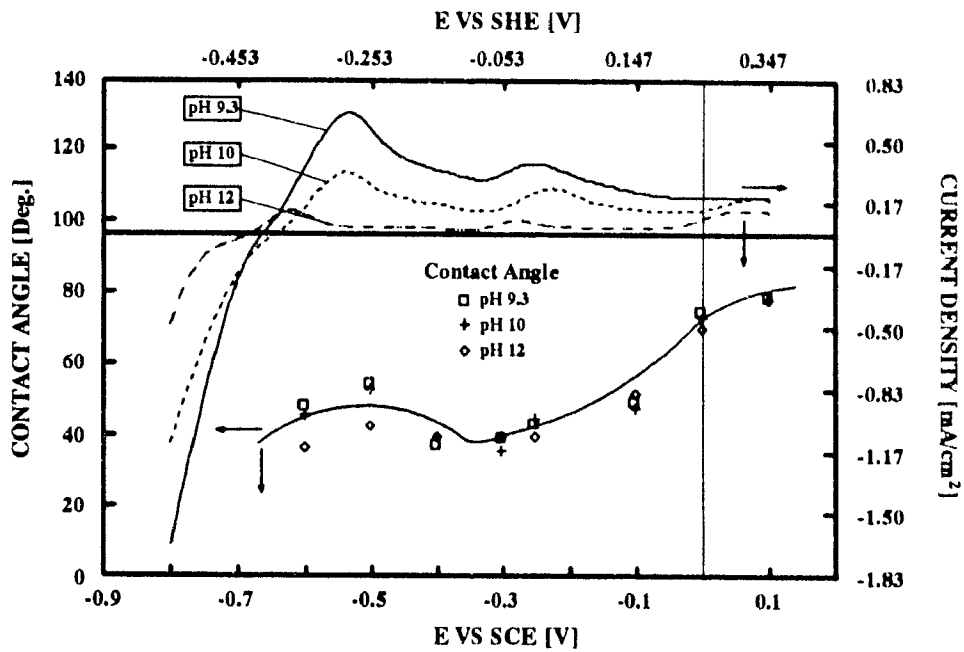


FIGURE 35. Contact angle and current density on chalcocite vs potential.

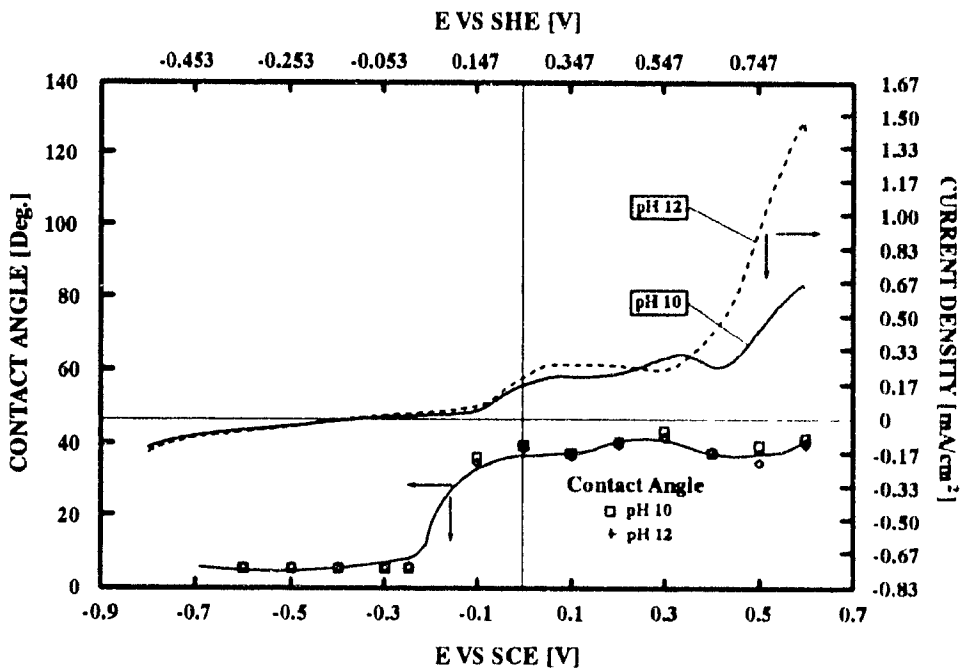


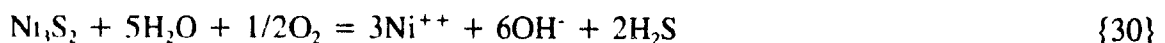
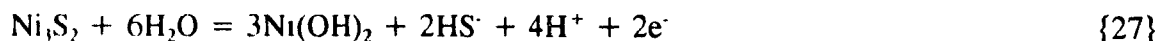
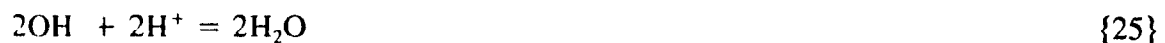
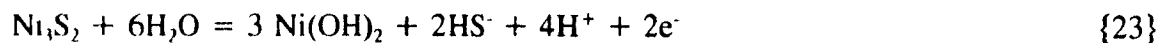
FIGURE 36 Contact angle and current density on heazlewoodite vs potential.

CHAPTER 4. DISCUSSION

4.1. DISSOLUTION:

As can be seen from Figures 7-10, Ni and Cu dissolution decreased with increasing pH and, for Ni, was essentially zero at pH 12. Also, from Figure 11, it is evident that there is significantly greater dissolution of heazlewoodite compared with chalcocite at pH 8. As is shown in Figure 12, in the presence of oxygen, the Ni concentration in solution is slightly higher than in the presence of air and nitrogen at pH 8. In the case of nitrogen, dissolution stabilizes after two hours. EDTA experiments show that, the dissolution increases significantly in the presence of EDTA as compared to that without EDTA (Figure 13).

The following reactions are proposed to explain dissolution of heazlewoodite



The overall reaction corresponds to the observed decrease in Ni concentration at elevated

CHAPTER 4. DISCUSSION

pH (the increase in OH⁻ concentration drives the reaction from right to left). In the presence of EDTA, dissolution is favoured because of the formation of a Ni-EDTA complex and removal of Ni hydroxy products from the surface [62].

It is interesting to note that flotation of matte is conducted under strongly alkaline condition (pH 12.4) [63] at which Ni dissolution from heazlewoodite is suppressed

4.2. REST POTENTIAL:

There is a significant difference between the rest potential of chalcocite and heazlewoodite at low pH values. However, the difference is suppressed as the pH increases towards the alkaline region and becomes negligible at pH 12 (Figures 14 and 15). This suggests the possibility of galvanic interaction between the minerals at acidic pH values but not at alkaline pH.

In the presence of collectors (2×10^{-3} M NaEX and MBT), the rest potential values of chalcocite are quite different as compared to heazlewoodite under similar conditions (Figures 16-19). This suggests that the interaction of collector with chalcocite is more extensive than with heazlewoodite. Also, it is noted from Figures 16-19 that the rest potential values in the presence of both NaEX and MBT are quite similar.

CHAPTER 4. DISCUSSION

4.3. CYCLIC VOLTAMMETRY

Chalcocite (Figures 22-27).

In the absence of collector (Figures 22-25);

• First anodic peak (A_1); the similarity with published data at pH 9.3 is shown by comparing Figures 22 and 23. Reactions have been proposed for the A_1 peak by Yoon et al. [54, 55] and Walker et al. [53]

The reaction suggested by Yoon et al. is,



$$E_h = -0.3 - 0.059 \text{ pH} \quad (11)$$

On substituting pH values 9.3, 10 and 12 in Equation (11), the E_h values did not correspond to the E_h values obtained from Figures 23-25 (Table 8).

The reaction suggested by Walker et al. is,



CHAPTER 4. DISCUSSION

$$E_h = -0.476 - 0.0295 \log [HS] + 0.0295 pOH \quad (12)$$

This second reaction fitted the observations (Table 8). It also corresponded to the reverse reaction of the second cathodic peak (K₂).

Table 8. Comparison of measured and calculated E_h for chalcocite (Anodic Peak A₁)

pH	E _h (V)		
	Yoon et al [21]	Walker et al [19]	Measured + 20mV
9.3	-0.85	-0.34	-0.36
10	-0.89	-0.36	-0.38
12	-1.01	-0.42	-0.43

- Second anodic peak (A₂); electrochemical measurements by Sato (56) suggest that the oxidation reaction of chalcocite in acid solution is represented by,



$$E_h = 0.53 + 0.0295 \log [Cu^{2+}] \quad (13)$$

CHAPTER 4. DISCUSSION

As can be seen, Equation (13) depends on the cupric ion activity in solution. It is given in basic solution by [56],

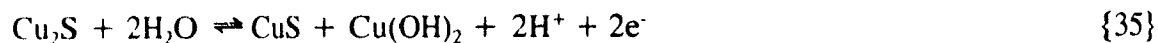


$$\log [\text{Cu}^{2+}] = 9.2 - 2 \text{ pH} \quad (14)$$

Substituting the value for cupric ion activity in Equation (13) gives,

$$E_h = 0.802 - 0.0591 \text{ pH} \quad (15)$$

Equation (15) represents the overall reaction 33 and 34,



When the pH values 9.3, 10 and 12 were substituted in Equation (14), the calculated E_h values fitted the measured values from Figures 23-25 (Table 9). The reverse reaction to this anodic peak (A₁) is the cathodic reaction K₁. As can be seen in Figure 25, this reaction shows strong reversibility at pH 12.

CHAPTER 4. DISCUSSION

Table 9. Comparison of measured and calculated E_h for chalcocite (Anodic Peak A_2)

pH	E_h (V)	
	Calculated	Measured ± 20 mV
9.3	0.25	0.26
10	0.21	0.23
12	0.09	0.09

In the presence of collector (2×10^{-3} M NaEX and MBT)(Figures 23-28);

- First anodic peaks (A_{1X}) (Figures 23-25) and (A_{1M}) (Figures 26, 27); these peaks are similar to the first anodic peaks without collector; however, they could be reactions with NaEX and MBT. This peak was also found by Mielczarski et al. [46] in the presence of KEX. They suggested the peak may be due to oxidation of hydrosulfide ions (i.e. Equation 2) which can form due to reduction of the cuprous sulfide or from xanthate decomposition, as was recently reported for a chalcocite/xanthate system in alkaline solutions [47]. It is suspected that hydrosulfide ions come mainly from xanthate decomposition.

- Second anodic peak (A_{2X}); the reaction for this has been proposed by Walker et al. (49) and Roos et al. [52],



CHAPTER 4. DISCUSSION

$$E_h = -0.171 - 0.0591 \log [X^-] \quad (16)$$

Substituting the concentration of xanthate ion (2×10^{-3} M) in Equation 16, gives -0.012 V which is in reasonable agreement with the value from Figures 23-25. The reverse of this reaction corresponds to the first reduction peak (K_{1X}) near -0.35 V,

$$E_h = -0.171 + 0.0591 \log [X^-] \quad (17)$$

• Second anodic peak (A_{2M}) (Figure 26) and third anodic peak (A_{2M}) (Figure 27); a possible reaction is,



with an E_h value around -0.060 V.

• Third anodic peaks (A_{1X}) (Figures 23-25), (A_{3M}) (Figure 26) and (A_{4M}) (Figure 27); in the presence of EX the second anodic peak observed in the absence of collector is significantly reduced, perhaps because the collector coating inhibits further oxidation of the mineral (48). The same argument can be applied to the third anodic reaction (A_{3M}) (Figure 26) and the fourth anodic reaction (A_{4M}) (Figure 27).

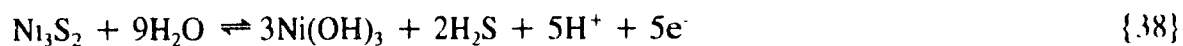
CHAPTER 4. DISCUSSION

- Third anodic peak (A_{3M}) (Figure 27); this reaction was not identified.

Heazlewoodite (Figures 28-31)

In the absence of collectors;

- Anodic peak (A_1); a possible reaction is [64],



$$E_h = 1.351 - 0.0591 \text{ pH} \quad (18)$$

The comparison of calculated and measured E_h values (Figure 29) is given in Table 10.

Table 10. Comparison of measured and calculated E_h for heazlewoodite (Anodic Peak A_1)

pH	E_h (V)	
	Calculated	Measured ± 20 mV
10	0.76	0.75
12	0.64	0.70

CHAPTER 4. DISCUSSION

In the presence of collectors;

- Anodic peaks (A_{1x}) and (A_{2x}), two weak anodic peaks were observed at pH 10 (Figure 27). In the case of xanthate the first one (A_{1x}) occurred around 0.30 V which probably corresponds to dixanthogen formation [58]. The second one (A_{2x}) was found around 0.55 V and was not identified. The weak peak (A_{1x}) was also found at pH 12 Figure (21). In general, similar voltammograms were found in the presence of MBT (Figures 30, 31).

4.4. CONTACT ANGLE:

No contact angle was found on either chalcocite or heazlewoodite in the absence of NaEX. There is a significant difference between contact angle values of chalcocite and heazlewoodite (Figures 33 and 34). The contact angle on heazlewoodite is zero at potentials lower than 0.15 V (-0.1 V SCE), while it is around 45° for chalcocite in the same potential region. Above 0.15 V heazlewoodite shows a steady contact angle around 40°; for chalcocite the contact angle increases to reach about 80° [46]. These findings suggest that selective flotation between the two minerals could be achieved with a controlled potential particularly at less than 0.15 V.

As shown in Figure 35, there is agreement between the cyclic voltammograms and contact angle measurements for chalcocite. According to the contact angle measurements hydrophobicity, and hence xanthate adsorption, begins at -0.35 V. The angle increases to 80°

CHAPTER 4. DISCUSSION

at 0.35 V corresponding to the disappearance of the anodic peak (A_1) in water alone. Thus, the surface product which passivated the chalcocite at these potentials is also hydrophobic.

Contact angle measurements were attempted with MBT; however, no bubble contact could be established.

CHAPTER 5. CONCLUSIONS

5.1. DISSOLUTION

- 1.- Ni (and some Cu) dissolution from matte was found. The dissolution decreased with increasing pH from 8 to 10 and became zero at pH 12.
- 2.- Cu dissolution from chalcocite was not as significant as Ni dissolution from heazlewoodite at pH 8
- 3.- Ni dissolution from heazlewoodite is slightly higher in oxygen-saturated than in air-saturated and nitrogen-saturated solutions.
- 4.- In the presence of EDTA significant additional dissolution of Ni was observed from heazlewoodite.
- 5.- A mechanism of heazlewoodite dissolution was proposed.

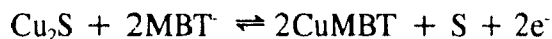
5.2. REST POTENTIAL

- 1.- Galvanic interaction between chalcocite (as the cathode) and heazlewoodite (as the anode) occurred at moderate pH but was zero at pH 12.
- 2.- The calculated and measured rest potentials are in a good agreement at different pH values.
- 3.- The effect of collectors on chalcocite is more significant than on heazlewoodite.
- 4.- The rest potential values of the minerals were quite similar in the presence of either NaEX or MBT.

CHAPTER 5. CONCLUSIONS

5.3. CYCLIC VOLTAMMETRY

- 1.- The two minerals showed significant differences in their electrochemical behaviour both in the presence and absence of collectors.
- 2.- The voltammograms suggest that NaEX and MBT interact with both minerals in a similar manner.
- 3.- The interaction of NaEX and MBT with heazlewoodite is not as significant as with chalcocite.
- 4.- NaEX and MBT created a surface product at 0.25 V which passivated the chalcocite.
- 5.- Most reactions for chalcocite and heazlewoodite were identified. For MBT, the following new reaction is proposed at $E_h = -0.060$ V,



5.4. CONTACT ANGLE

- 1.- Contact angle measurements suggested that xanthate interaction with chalcocite began at potentials as low as ~ -0.35 V.
- 2.- Measurements showed that there was a significant difference between contact angle values of chalcocite and heazlewoodite.
- 3.- There was agreement between cyclic voltammograms and contact angle measurements

CHAPTER 5. CONCLUSIONS

4.- In the presence of NaEX the surface product which passivated the chalcocite at 0.25 V was strongly hydrophobic.

5.- Contact angles were zero with MBT.

References

- [1] Woods, R., 1972. "Electrochemistry of Sulphide Flotation". Aust Inst Min Met , No 241, pp. 53-61.
- [2] Woods, R., 1976 "Electrochemistry of Sulphide Flotation" Chapter 10 in Principles of Mineral Flotation. Gaudin Memorial Volume. Edited by M C. Fuerstenau, Published by AIME, pp. 298-333.
- [3] Woods, R., 1984. "Electrochemistry of Sulphide Flotation". Chapter 3 in Principles of Mineral Flotation. The Wark Symposium, Edited by M.H Jones and J.T. Woodcock, Published by AIMM, pp. 91 115
- [4] Ralston J., 1991. " E_h and Its Consequences in Sulphide Mineral Flotation". Miner. Eng , Vol 4, pp. 859-878.
- [5] Macpherson, A.R. and Turner, R.R., 1978. "Autogenous Grinding from Test Work to Purchase of a Commercial Unit". Chapter 13 in Mineral Processing Plant Design. Edited by A.L. Mular and R.B. Bhappu. Published by SME-AIME, pp 286
- [6] Lo, W.W , Surges, L.J. and Hancock, H.A , 1985. "The Preferential Aqueous Oxidation of Sphalerite in a Mixed Sulphide Tailing Using Manganese Dioxide Complex Sulphides Processing of Ores, Concentrates and By Product". Published by TMS-AIME, pp 907-923.
- [7] Mizoguchi, T. and Habashi, F., 1983. "Aqueous Oxidation of Zinc Sulphide, Pyrite and Their Mixtures in Hydrochloric Acid". Trans. Instn Min Metall , Section C, pp 14-19
- [8] Learmont, M.E. and Iwasaki I , 1984. "The Effect of Grinding Media on Galena Flotation". Min. and Met. Proc., Vol 2, pp 136-143
- [9] Nakazawa, H. and Iwasaki, I , 1985 "Effect of Pyrite-Pyrrhotite Contact on Their Floatabilities". Min. and Met. Proc., Vol 2, pp 206-211
- [10] Guy, P.J. and Trahar W.I., 1985 "The Effects of Oxidation and Mineral Interaction on Sulphide Flotation". Flotation of Sulphide Minerals Edited by K.S.E. Forssberg

References

- Published by Elsevier, pp. 91-110
- [11] Yoon, R H , 1981 "Collectorless Flotation of Chalcopyrite and Sphalerite Ores Using Sodium Sulphide" Int J Miner. Process., Vol. 8, pp. 31-48.
- [12] Trahar, W J , 1983. "A Laboratory Study of the Influence of Sodium Sulphide and Oxygen on the Collectorless Flotation of Chalcopyrite". Int. J. Miner. Process., Vol. 11, pp. 57-74.
- [13] Lepetic, V.M., June 1974. "Flotation of Chalcopyrite Without Collector After Dry Autogenous Grinding". CIM Bull., pp. 71-77.
- [14] Gebhardt, J.E., Dewnsnap N F. and Richardson, P.E., 1985. "Electrochemical Conditioning of a Mineral Particle Bed Electrode for Flotation". U. S. Bureau of Mines Rept. Inv. 8951
- [15] McTavish, S., 1985 "Goldstream Concentrator Desing and Operation". Proceedings 17th Annual Meeting of the Canadian Mineral Processors, Ottawa, pp. 61-79.
- [16] Sutherland, K L. and Wark, I.W., 1955. "Principles of Flotation". Published by AIMM, pp 232.
- [17] Ref 16, pp. 103.
- [18] El-Shall, H., Zucker, G. and Lafftus, K., 1984. "Electrochemical Surface Properties of Molybdenite". Electrochemistry in Minerals and Metal Processing. Edited by P.E. Richardson, S. Srinivason and R Woods. Published by The Electrochemical Society, pp. 96-111.
- [19] Gaudin, A M., Miaw, H.L. and Spedden, H.R., 1957. "Native Floatability and Crystal Structure". Proceedings of 2nd Int. Congress of Surface Activity, Edited by J.H. Schulman. Published by Butterworth, London, pp. 202-219.
- [20] Fuerstenau, M C and Sabacky, B.J., 1981. "On the Natural Floatability of Sulphides". Int. J. Miner. Process., Vol. 8, pp. 79-84.

References

- [21] Chen, K.Y. and Morris, J.C., 1972 "Kinetic of Oxidation of Aqueous sulphide by Oxygen". *Environmental Sci. Tech*, Vol 6, pp 529-537
- [22] Gardner, J.R. and Woods, R., 1979. "An Electrochemical Investigation of the Natural Floatability of Chalcopyrite" *Int. J. Miner. Process*, Vol 6, pp. 6-16.
- [23] Majima, H., 1969. "How Oxidation Effects Selective Flotation of Complex Sulphide Ores". *Can. Metall. Quart.*, Vol. 8, pp. 269-273
- [24] Martin, C.J., McIvor, R.E., Finch J.A. and Rao S.R., 1991 "Review of the Effect of Grinding Media on the Flotation of Sulphide Minerals". *Minerals. Eng.*, Vol. 4, pp. 121-132.
- [25] Kocabağ, D. and Smith, M.R., 1985. "The Effect of Grinding Media in the Flotation of Sulphide Minerals". In *Complex Sulphides*. Edited by A.D. Zunkel, R.S. Boorman, A.E. Morris and Wesley R.J.. The Metallurgical Society, pp 55-82
- [26] Labonte, G., 1987 "Electrochemical Potentials in Flotation Systems Measurement Interpretation and Applications". Master Thesis, Mining & Metallurgical Eng. Department, McGill University
- [27] Adam, K. and Iwasaki, I., 1984 "Pyrrhotite-Grinding Media Interaction and Its effect on Floatability at Different Applied Potentials". *SME-AIME Annual Meeting*, pp 84-89
- [28] Pozzo, R.L., Malicsi, A.S. and Iwasaki, I., 1990. "Pyrite-Pyrrhotite Grinding Media and Its Effect on Flotation". *Min. and Met. Proc*, Vol 7, pp 16-21
- [29] Rao, S.R. and Finch, J.A., 1987. "Electrochemical Studies on the Flotation of Sulphide Minerals with Special Reference to Pyrite-Sphalerite". *Can. Metall. Quart.*, Vol 26, pp 173-175.
- [30] Rao, S.R. and Finch, J.A., 1988. "Galvanic Interaction Studies on Sulphide Minerals" *Can. Metall. Quart.*, Vol. 26, pp. 253-259.
- [31] Martin, C.J., Rao, S.R., Finch J.A. and Leroux, M., 1989. "Complex Sulphide Ore

References

- Processing with Pyrite Flotation by Nitrogen". *Int J Miner. Process.*, Vol. 26, pp. 95-110
- [32] Sandoval-Caballero, I , Leroux, M., Rao, S R and Finch J.A., 1990. "Nitrogen Flotation of Pyrite in a Continuous Minicell at Brunswick Mining". *Minerals Eng.*, Vol. 3, pp. 369-373
- [33] Johnson, N W , 1988 "Application of Electrochemical Concepts to Four Sulphide Flotation Separations". *Electrochemistry in Mineral and Metal Processing II*. Edited by P E. Richardson and R Woods, Published by The Electrochemical Society, pp. 131-145.
- [34] Wilson, S W , Kolez, H , Dobby, G. and Stratton-crawley, R., 1990. "Flotation Column Scale-Up at INCO's Matte Separation Plant". Presented at the 22nd Annual Operators Conference of the Canadian Mineral Processor Division of CIM, pp. 218-241.
- [35] Boldt, J R , 1967 "The Wining of Nickel". Edited by P. Queneau, Published by Longman Canada Ltd, Toronto, pp. 275-276.
- [36] Greef, S , Peat, R., Peter, L M , Pletcher, D. and Robinson, J., 1985. "Instrumental Methods in Electrochemistry" Published by Ellis Horwood Ltd., England, pp. 22-23.
- [37] Lide, D R , 1992-1993 "Handbook of Chemistry and Physics" Published by CRC Press Inc., 73rd Edition, section 5, pp. 8-50.
- [38] Garrels, R M and Christ C.L , 1965. "Solution, Minerals and Equilibria". Published by Harper & Row, New York
- [39] Chander, S , 1988 "Electrochemistry of Sulphide Mineral Flotation". *Min. and Met. Process* , Vol 5, pp 104-114.
- [40] Fuerstenau, M C , Miller, I.D , and Kuhn, M.C., 1985. "Chemistry of Flotation". Published by AIME, New York, pp. 115-118.
- [41] Bard, A.J , 1980 "Electrochemical Methods Fundamental and Applications". Published by John Wiley and Sons Inc., pp. 24-25.

References

- [42] Wassos, B.H. and Ewing, G.W., 1983. "Electroanalytical Chemistry" Published by John Willey & Sons Inc , pp. 37-39.
- [43] Ref. 35, pp. 178-182.
- [44] Ref. 40, pp. 137.
- [45] Heyes, G.W. and Trahar, W.J , 1979. "Oxidation-Reduction Effects in the Flotation of Chalcocite and Cuprite". Int. J. Miner Process , Vol 6, pp 229-252.
- [46] Mielczarski, J.A., Zachwieja, J.B. and Yoon, R.H., 1990. "The Dual Role of Xanthate in the Induction of Hydrophobicity of Chalcocite". SME-AIME Annual Meeting, Salt Lake City, UT, Preprint No. 90-174.
- [47] Mielczarski, J.A., Zachwieja, J.B. and Yoon R.H , 1991. "Structure of Surface Layers on Cuprous Sulphide Electrodes In Xanthate Solution" Submitted for Publication (copy provided by Yoon).
- [48] O'Dell, C.S., Dooley, R.K., Walker, G.W and Richardson, P E., 1985 "Chemical and Electrochemical Reactions in the Chalcocite-Xanthate System" Electrochemistry in Mineral and Metal processing" Edited by P.E. Richardson, S Srinivason and R Woods, pp 81-95.
- [49] Pritzker, M.D., Yoon, R H., Basilio, C. and Choi, W.Z., 1985 "Solution and Flotation Chemistry of Sulphide Minerals". Canadian Metal. Quart., Vol 24, pp 27-38
- [50] Richardson, P.E , Stout, J V., Proctor, C L. and Walker, G W , 1984 "Electrochemical Flotation of Sulphides: Chalcocite-Ethylxanthate Interactions" Int. J. Miner. Process., Vol 12, pp. 73-93.
- [51] Richardson, P E and Walker, G W , 1985 "The Flotation of Chalcocite, Bornite, Chalcopyrite, and Pyrite in an Electrochemical-Flotation Cell" XV Int. Miner. Process Congr 2, pp. 198-210.
- [52] Roos, J.R., Celis, J.P. and Sudarsono, A S., 1990. "Electrochemical Control of

References

- Chalcocite and Covellite-Xanthate Flotation" *Int. J. Miner. Process.*, Vol. 29, pp. 17-30.
- [53] Walker, G W , Stout, J V and Richardson, P E , 1984. "Electrochemical Flotation of Sulphides: Reactions of Chalcocite in an Aqueous Solution". *Int. J. Miner. Process.*, Vol. 12, pp. 55-72
- [54] Woods, R , Young, C A and Yoon, R H , 1990. "Ethylxanthate Chemisorption Isotherms and E_h -pH Diagrams for the Copper/Water/Xanthate and Chalcocite/Water/Xanthate Systems" *Int. J. Miner. Process.*, Vol. 30, pp. 17-33
- [55] Woods, R , Young, C A , and Yoon R.H., 1988. "A Voltammetric Study of Chalcocite Oxidation to Metastable Copper Sulphides" *Electrochemistry in Mineral and Metal Processing*. Edited by P.E Richardson and R, Woods. Published by The Electrochemical Society, pp. 3-17.
- [56] Latimer, W M , 1952 "The Oxidation States of the Elements and Their Potentials in Aqueous Solution" Published by Prentice-Hall Inc., New York, pp. 392.
- [57] Sato, M , 1960 "Oxidation of Sulphide Ore Bodies, II. Oxidation Mechanisms of Sulphide Minerals at 25°C" *Leon. Geo.*, Vol. 55, pp. 1202-1231.
- [58] Critchley, J K and Hunter, C J , 1987 "Development of Contact Angles on Heazlewoodite" *Trans. Instn. Min. Metall., Sect. C*, Vol. 96, pp. 166-168.
- [59] Dean, J A , 1985 "Lange's Hand Book of Chemistry" Published by McGraw-Hill Book Comp., New York, Thirteenth Edition, Sect. 5, pp. 99-105
- [60] Mieleczarski, J A and Yoon, R.H , 1989 "Fourier Transform Infrared External Reflection Study of Molecular Orientation in Spontaneously Adsorbed Layers on Low-Absorption Substrates". *J. Phys. Chem.*, Vol. 93, No. 5, pp. 2034-2038.
- [61] Kelebek, Ş, 1980 "Surface Chemistry of Coal Flotation Systems". Master Thesis, Mining & Metallurgical Eng. Department, McGill University, pp. 127
- [62] Senior, G.D. and Trahar, W J , 1991. "The Influence of Metal Hydroxides and Collector

References

- on the Flotation of Chalcopyrite". *Int. J. Miner. Process* , Vol 33, pp 321-345
- [63] Tipman, N.R., Agar, G.E. and Pare, L , 1976 "Flotation Chemistry of the INCO Matte Separation Process" *Flotation, A.M. Gaudin Memorial Volume, Vol. 1, Chapt 18*, pp 528-548.
- [64] Hodgson M. and Agar G.E., 1985. "Electrochemical and Flotation Studies on Pyrrhotite and Pentlandite". 114th Meeting AIME, New York.